A fuzzy and random moment-based arbitrary polynomial chaos method for response analysis of composite structural-acoustic system with multi-scale uncertainties

Wenqing Zhu[1], Yingbin Hu[1], Ning Chen[1,*] , Jian Liu[1], Michael Beer[2,3,4]

[1]State Key Laboratory of Advanced Design and Manufacturing for Vehicle Body, Hunan University, Changsha, Hunan, 410082, People's Republic of China

[2] Institute for Risk and Reliability, Leibniz University Hannover, Callinstr. 34, 30167 Hannover, Germany

[3] Institute for Risk & Uncertainty, School of Engineering, University of Liverpool, Brodie Tower, Brownlow Street, Liverpool L69 3GQ, United Kingdom

[4] School of Civil Engineering & International Joint Research Center for Engineering Reliability and Stochastic Mechanics, Tongji University, China

Abstract: A new unified polynomial chaos expansion method, named as *fuzzy and random moment-based arbitrary polynomial chaos method* (FRMAPCM), is proposed for the response analysis of the composite structural-acoustic system with multi-scale fuzzy/bounded random uncertainties. In the FRMAPCM, the *moment-based arbitrary polynomial chaos* (MAPC) is adopted to construct the polynomial basis according to the moment of the bounded random variable. The coefficient of MAPC is calculated by using the Gauss integration method. For the fuzzy variable, the weight function of the Chebyshev polynomial is assumed as the *probability density function* (PDF) to

yield the moment matrix. Compared with the conventional polynomial based method which constructs the polynomial basis according to the PDF of the random variable, the proposed FRMAPCM can avoid the error produced by the process of approximating the PDF. A numerical example is given to validate the proposed method, and two engineering examples are presented to demonstrate its efficiency and accuracy.

Key Words: Composite structural-acoustic system; Fuzzy and bounded random variables; Multi-scale uncertainties; Moment-based arbitrary polynomial chaos method

1. Introduction

Composite materials are widely used in the automotive and aerospace industries because of their excellent functional properties. However, thin, lightweight, and flexible composite panels are vulnerable to vibration and can radiate noise into passenger compartments when excited by a dynamic force. The vibration can be more severe when resonance occurs. Therefore, it is important to conduct vibro-acoustic analysis on structural-acoustic systems involving composite materials. In practice, the microstructural parameters of composite materials are often uncertain because of inevitable manufacturing errors and incomplete knowledge. The vibro-acoustic analysis results may be unreliable if those involved uncertainties are ignored. Therefore, those uncertainties need to be taken into consideration mathematically during conducting vibro-acoustic analysis. In general, based on the sources of uncertainty, uncertainty can be divided into epistemic and aleatory categories [1]. The

epistemic uncertainty is related to incomplete or inaccurate information in any activity at the modeling process and can be reduced by gathering more knowledge or experimental data. On the other hand, the aleatory uncertainty comes from the inherent variation of the physical system or environment, which is usually modeled as random variable using probability theory. For random system response analysis, many numerical methods have been developed, such as the *Monte Carlo method* (MCM) [2], the stochastic perturbation method [3-5] and the random polynomial expansion method [6-9] and so on. However, random model is inappropriate for the epistemic uncertainty, since even small deviation from the real *probability density function* (PDF) may lead to relatively large error of the statistic response [10]. In practical engineering, it is difficult to acquire enough data to define the distribution parameters of the random model accurately. Therefore, for an uncertain parameter whose exact probability distribution is difficult to acquire, the non-probabilistic model [11] can be used to describe its uncertainty as an alternative. In comparison to the aleatory uncertainty analysis, the quantification of epistemic uncertainty could be more challenging. Many non-probabilistic or imprecise probabilistic uncertain methods have been proposed to quantify the epistemic uncertainty in a more effective way, such as the fuzzy set [12-16], the possibility theory [17], the interval model [18, 19] and the evidence theory [20]. Interval model can be used to model uncertain parameters whose lower and upper bounds are well defined but information about their probability density functions is missing [21]. Due to the interval model is only a λ-cut of fuzzy number, it belongs to the category of fuzzy model. Thus, with enough

information acquired, fuzzy model can better describe the uncertainty than the interval model. In practical engineering, different kind of uncertainties may exist simultaneously. Therefore, it is necessary to build the hybrid uncertain model to contain both aleatory uncertainty and epistemic uncertainty [22-25]. The most commonly used one is the hybrid interval and random model [26], which has been extensively applied in many engineering fields. However, since the interval model is a special case of the fuzzy model [27], the hybrid model including fuzzy variables and random variables may be more typical than the hybrid interval and random model for dealing with the uncertain problem involving aleatory uncertainty and epistemic uncertainty.

As for composite structural-acoustic systems, multi-scale uncertainties exist simultaneously. At the micro-scale, the uncertainty may come from the constituent material properties of the microstructure due to manufacturing errors. The source of the uncertainties at the macro-scale is from the physical parameters of the acoustic medium and the external load resulting from the environment. Both the uncertainties from the micro-scale and the uncertainties from the macro-scale can influence the frequency response of the composite structural-acoustic system. Thus, multi-scale uncertainties should be considered when analyzing composite structural-acoustic systems. Chen at al. proposed an *evidence-theory-based polynomial expansion method* (EPEM) for dealing with the composite structural–acoustic problem involving multi-scale mixed aleatory and epistemic uncertainties [28]. In the EPEM, interval variables and random variables are transformed into evidence variables appropriately,

which can bring high efficiency without losing accuracy. Besides, a *homogenization-based Gegenbauer polynomial expansion method* (HGPEM) was developed for response analysis of multi-scale hybrid uncertain composite structural-acoustic system [29]. From the overall perspective, research on composite structural-acoustic system with multi-scale uncertainties is meaningful and promising but still on its preliminary stage. The composite structural-acoustic system with multi-scale fuzzy and random uncertainties has not been touched upon yet, especially when only the statistical data of the random variables in the mixed fuzzy and random model is available.

For linear dynamical system with random and fuzzy uncertainties, E. Jacquelin et al. have developed a general framework to derive its response by employing the *generalized polynomial chaos method* (gPCM) [30]. The *generalized polynomial chaos* (gPC) was developed by employing orthogonal polynomial from the Askey scheme to establish the polynomial chaos expansion [31], which has been widely used in practical engineering due to the ease of the construction of polynomial basis. For example, Yin et al. proposed an *evidence-theory-based Jacobi expansion method* (ETJEM) which permits a much wider choice of polynomial bases to control the error of approximation than the traditional evidence-theory-based orthogonal polynomial approximation method [20]. Gao et al. proposed an *improved Jacobi chaos expansion method* (IJCEM) for response analysis of the finite element system with bounded random variables following arbitrary probability distributions [32]. Qiu et al. proposed a novel efficient and accurate approach to crack propagation analysis

in structures with random uncertainties based on *polynomial chaos expansion* (PCE) method [33]. Xu et al. proposed a dual-layer dimension-wise fuzzy finite element method for the structural-acoustic analysis with epistemic uncertainties through orthogonal polynomial approximation [34]. However, in the gPCM, the orthogonal polynomial from the Askey scheme can only provide the optimal polynomial basis for some well-known distribution. For the random problems with complex probability distribution, the *Gegenbauer series expansion method* (GSEM) need to approximate its PDF with λ-PDF [35], while a nonlinear variable transformation should be taken in gPCM [36]. This kind of approximation or transformation will cause error. Therefore, accuracy of GSEM and gPCM may be deteriorated. The aim of this paper is to propose a new unified polynomial chaos expansion method for the response analysis of the composite structural-acoustic system with multi-scale fuzzy/bounded random uncertainties, where only the sampling points data of the random variables can be acquired. To overcome the drawbacks of gPCM as mentioned above, the random arbitrary polynomial chaos method for random problems with arbitrary PDF is introduced and adopted in this paper [37, 38]. By applying *moment-based arbitrary polynomial chaos* (MAPC) on random analysis and extending it for fuzzy analysis, a new unified method is proposed, named as the *fuzzy and random moment-based arbitrary polynomial chaos method* (FRMAPCM). In the FRMAPCM, the MAPC constructs polynomial basis according to the moment of bounded random variable. The coefficient of MAPC is calculated by using the Gauss integration method. For fuzzy variable, the weight function of the Chebyshev polynomial is assumed as the

PDF to yield the moment matrix and then uses it to construct the polynomial basis. Compared with the traditional gPC, the MAPC employed in the proposed method can construct optimal polynomial basis for arbitrary probability distribution. Furthermore, the MAPC can avoid the error produced by approximating the PDF of bounded random variable.

2. The homogenization-based finite element method (HFEM) for the composite structural-acoustic system

In this paper, the case we examine is a plate constructed with periodic microstructures, which is coupled with an acoustic cavity. Both the plate and the acoustic medium satisfy the linear constitutive equations and it is assumed that the acoustic medium is inviscid and incompressible. The fluid just exerts normal loads on the structure and only the normal displacement of the structure is coupled with the fluid on the interface between the structure and the fluid. The external excitation is assumed to be time harmonic. The HFEM can be divided into two steps: First, obtaining equivalent material properties of the microstructure at macro-scale by conducting the homogenization analysis; Secondly, using the macro equivalent material properties to conduct the coupled FEM/FEM analysis of the composite structural-acoustic system.

The dynamic equilibrium equation of the composite structural–acoustic system in the time domain can be expressed as

$$\begin{bmatrix} \mathbf{M}_s & 0 \\ \rho_f \mathbf{H}^T & \mathbf{M}_f \end{bmatrix} \begin{Bmatrix} \ddot{\mathbf{u}}_s \\ \ddot{\mathbf{p}} \end{Bmatrix} + \begin{bmatrix} \mathbf{C}_s \\ 0 \end{bmatrix} \begin{Bmatrix} \dot{\mathbf{u}}_s \\ \dot{\mathbf{p}} \end{Bmatrix} + \begin{bmatrix} \mathbf{K}_s & -\mathbf{H} \\ 0 & \mathbf{K}_f \end{bmatrix} \begin{Bmatrix} \mathbf{u}_s \\ \mathbf{p} \end{Bmatrix} = \begin{Bmatrix} \mathbf{F}_s \\ \mathbf{F}_f \end{Bmatrix} \tag{1}$$

where ρ_f is the density of the acoustic fluid; $\mathbf{K}_s$ and $\mathbf{M}_s$ stand for the composite

structural stiffness matrix and mass matrix; $\mathbf{C}_s$ is the structural damping matrix, $\mathbf{K}_f$ and $\mathbf{M}_f$ stand for the acoustic stiffness matrix and mass matrix; $\mathbf{H}$ is the spatial coupled matrix; $\mathbf{u}_s$ and $\mathbf{p}$ are the displacement amplitude vector of composite structure and the sound pressure amplitude vector in the acoustic domain; $\mathbf{F}_s$ and $\mathbf{F}_f$ are the generalized force vectors related to the composite structure and to the internal acoustic cavity.

Assumed the forces in Eq. (1) are time harmonic, and then the displacement and sound pressure response are time harmonic. Thus, in the frequency domain, one can get

$$\begin{bmatrix} \mathbf{K}_s + i\omega\mathbf{C}_s - \omega^2\mathbf{M}_s & -\mathbf{H} \\ \rho_f\omega^2\mathbf{H}^{\mathrm{T}} & \mathbf{K}_f - \omega^2\mathbf{M}_f \end{bmatrix} \begin{Bmatrix} \mathbf{u}_s \\ \mathbf{p} \end{Bmatrix} = \begin{Bmatrix} \mathbf{F}_s \\ \mathbf{F}_f \end{Bmatrix} \tag{2}$$

For simplicity, Eq. (2) can be expressed as

$$\mathbf{ZU} = \mathbf{F} \tag{3}$$

where $\mathbf{Z}$ is the composite structural-acoustic dynamic stiffness matrix; $\mathbf{U}$ is the frequency response vector; $\mathbf{F}$ is the external excitation vector. They can be expressed as

$$\mathbf{Z} = \begin{bmatrix} \mathbf{K}_s + i\omega\mathbf{C}_s - \omega^2\mathbf{M}_s & -\mathbf{H} \\ \rho_f\omega^2\mathbf{H}^{\mathrm{T}} & \mathbf{K}_f - \omega^2\mathbf{M}_f \end{bmatrix}, \quad \mathbf{U} = \begin{Bmatrix} \mathbf{u}_s & \mathbf{p} \end{Bmatrix}^{\mathrm{T}}, \quad \mathbf{F} = \begin{Bmatrix} \mathbf{F}_s & \mathbf{F}_f \end{Bmatrix}^{\mathrm{T}} \tag{4}$$

where ω is the angular frequency of external excitation. Here, it should be noted that the matrices and vectors are dependent on angular frequency as well as on the involved parameters. The detailed derivation of Eq. (4) is provided in Ref. [29].

The composite structural stiffness matrix $\mathbf{K}_s$ and mass matrix $\mathbf{M}_s$, can be expressed as

$$\mathbf{K}_s = \sum_{j=1}^{N_{cell}} \left(\int_{\Omega_j} \mathbf{B}^{\mathrm{T}} \mathbf{D}^{\mathrm{H}} \mathbf{B} \mathrm{d}\Omega \right) \tag{5}$$

$$\mathbf{M}_s = \sum_{j=1}^{N_{cell}} \int_{\Omega_j} \eta^{\mathrm{H}} \mathbf{N}_s^{\mathrm{T}} \mathbf{N}_s \mathrm{d}\Omega \tag{6}$$

where **B** is the strain matrix at the macroscale; $\mathbf{N}_s$ is the Lagrange shape function of the isoparametric quadrilateral element; the summation represents an assembly process of the system matrices and vectors; N_{cell} is the total number of elements in the structural domain; Ω_j is the jth element in the structural domain. $\mathbf{D}^{\mathrm{H}}$ is the equivalent macro constitutive matrix [39], η^{H} is the average mass density of the micro unit cell.

where the equivalent macro constitutive matrix $\mathbf{D}^{\mathrm{H}}$ of the microstructure can be calculated through the homogenization method

$$\mathbf{D}^{\mathrm{H}} = \frac{1}{|\Omega|} \int_{\Omega} \mathbf{D}_e \left(\mathbf{I} - \mathbf{b}\boldsymbol{\chi} \right) d\Omega \tag{7}$$

Here Ω is the domain of the micro unite cell and $|\Omega|$ represents its area; $\mathbf{D}_e$ stands for the constitutive matrix of the eth element in the micro unite cell; the symbol **I** is a unit matrix; the symbol **b** is the strain matrix at the micro scale; $\boldsymbol{\chi}$ represents the characteristic displacement of the microstructure. $\boldsymbol{\chi}$ satisfies the auxiliary equation which is expressed as

$$\mathbf{k}\boldsymbol{\chi} = \mathbf{f} \tag{8}$$

here, the stiffness matrix **k** and the force vector **f** of the micro unite cell at the micro-scale can be expressed as

$$\mathbf{k} = \int_{\Omega} \mathbf{b}^T \mathbf{D}_e \mathbf{b} d\Omega \tag{9}$$

$$\mathbf{f} = \int_{\Omega} \mathbf{b}^T \mathbf{D}_e d\Omega \tag{10}$$

in which the constitutive matrix $\mathbf{D}_e$ can be interpolated using the solid isotropic

material with penalization (SIMP) model, that is

$$\mathbf{D}_e = x_e^q \mathbf{D}^1 + \left(1 - x_e^q\right)\mathbf{D}^2 \tag{11}$$

where $\mathbf{D}^1$ and $\mathbf{D}^2$ stand for the constitutive matrices of the two given solid isotropic base material 1 and 2, respectively; x_e is the relative volumetric density, which describes the layout of the micro structure. The symbol q is the exponent of penalization, which usually is set as 3.

The average mass density η^{H} of the micro unit cell can be calculated straightforwardly as

$$\eta^{\mathrm{H}} = \frac{1}{|\Omega|}\int_{\Omega} \eta_e d\Omega \tag{12}$$

Here, η_e is the mass density of the eth element in the micro unit cell and can also be interpolated by the SIMP model with the exponent of penalization equals to 1, which can be expressed as

$$\eta_e = x_e \eta^1 + \left(1 - x_e\right)\eta^2 \tag{13}$$

where η^1 and η^2 stand for the mass density of the two given solid isotropic base material 1 and 2, respectively.

3. The hybrid model

In practical engineering problems, uncertainties in material properties, geometric dimensions, environmental parameters, and external loads are unavoidable. These uncertain parameters are always bounded because of the limitations in design tolerance. For the system with several uncertain parameters, we denote these parameters with a bounded vector $\mathbf{x} = \left[x_1, x_2, ..., x_L\right]$, which satisfies $\underline{\mathbf{x}} \le \mathbf{x} \le \overline{\mathbf{x}}$. The symbol L represents the number of uncertain parameters. In addition, the symbols

$\underline{\mathbf{x}}$ and $\overline{\mathbf{x}}$ respectively denote the lower and the upper bounds of **x**.

3.1. Bounded random variables

When the information is enough to construct the *probability density function* (PDF) precisely in the variation range [40], the bounded random model is a valuable mathematical model to treat the uncertain parameters in engineering practices. When the PDF of variable x_i is well defined, x_i can be modeled by a bounded random variable x_i^R and the bounded random variable x_i^R satisfies

$$\begin{cases} p(x_i^R) > 0, \ \ x_i^R \in [\underline{x}_i, \overline{x}_i] \\ p(x_i^R) = 0, \ \ \text{else} \end{cases} \tag{14}$$

where $p(x_i^R)$ is the PDF of x_i^R. It is noted here that the bounded random variables are a special case of random variables because its variation range is finite.

3.2. Fuzzy variables

When the information on the uncertain parameters is given in terms of intervals that reflect the possible values of these parameters, fuzzy model can be used [41]. Fuzzy variables are related to fuzzy sets $\overline{\Omega}$. It is defined by a set Ω and its membership function ε_Ω. ε_Ω is defined as

$$\begin{aligned} \varepsilon_\Omega : \mathrm{T} &\to [0,1] \\ x &\mapsto \varepsilon_\Omega(x) \end{aligned} \tag{15}$$

Where T is the set used to define the fuzzy variable and $\Omega \subset T$. Zadeh [42] proposed the concept of fuzzy sets and interpreted the membership function as the degree of possibility for a variable to belong to Ω (i.e. the degree of membership of x in Ω). The $\varepsilon_\Omega(x)$ equals to 0 when x does not belong to Ω, whereas $\varepsilon_\Omega(x)$ equals to 1 when x belongs to Ω. For some $x \in \Omega$, $\varepsilon_\Omega(x)$ is between 0 and 1,

which indicates that x possibly belongs to Ω and the degree of membership varies from weak to strong when $\varepsilon_{\Omega}(x)$ varies from 0 to 1. The support of $\bar{\Omega}$ can be depicted as

$$\text{supp}(\bar{\Omega}) = \{x \in T \,|\, \varepsilon_{\Omega}(x) > 0\} \tag{16}$$

A λ-cut is defined by

$$\Omega_{\lambda} = \{x \in T \,|\, \varepsilon_{\Omega}(x) \geq \lambda\} \quad \text{for } 0 < \lambda < 1 \tag{17}$$

The element of Ω_{λ} has a degree of membership greater or equal to λ.

In the fuzzy uncertainty propagation, the objective is to provide the interval I_{λ} whose bounds correspond to the minimum and maximum of the response for all λ-cuts. Thus, for each λ-cut, the extrema of the solution of Eq. (3) must be calculated over all values that belong to the λ-cut of the fuzzy variables.

3.3. Definition of the hybrid model

For a complex engineering system, different type of uncertain parameters may exist simultaneously. In this paper, the considered case includes bounded random variables and fuzzy variables, which exist in structural-acoustic systems simultaneously and independently. The bounded random model is used to handle the parameters whose PDFs are defined unambiguously due to sufficient information. However, we can't get the precise PDF of uncertain parameter in most situations because of insufficient information or knowledge. When the information on the uncertain parameters is given in terms of intervals that reflect the possible values of these parameters, the fuzzy model can be used. The hybrid model containing bounded random variables and fuzzy variables can be expressed as

$$\mathbf{x} = [\mathbf{x}^R, \mathbf{x}^F] = [x_1^R, x_2^R, ..., x_{L_1}^R, x_{L_1+1}^F, ..., x_L^F] \tag{18}$$

Where, x^R denotes bounded random variable, x^F denotes fuzzy variable.

4. Hybrid uncertain analysis method

The *generalized polynomial chaos* (gPC) can only achieve good efficiency for uncertainty with the *probability density function* (PDF) in the Askey scheme. Besides, it is effective only when the PDF is available. The *moment-based arbitrary polynomial chaos* (MAPC) is proposed based on gPC. It can be conducted without knowing the PDF of random variable. Moreover, the MAPC can be used for any distribution. In this section, the MAPC is introduced into composite structural-acoustic problem with multi-scale fuzzy/bounded random uncertainties. More details about MAPC can be found in Ref. [38].

4.1. Moment-based arbitrary polynomial chaos approximation

Using the sums of orthogonal polynomials of independent variables to approximate the uncertain process of interest is the basic idea of polynomial chaos expansion. The polynomial chaos expansion to approximate a function can be expressed as follows

$$Y(\xi) = \sum_{i=0}^{N} y_i \varphi_i(\xi) \tag{19}$$

Where N is the retained order of *arbitrary polynomial chaos* (APC) expansion, y_i denotes the expansion coefficient to be estimated, $\varphi_i(\xi)$ represents the polynomial basis of order *i*. $\varphi_i(\xi)$ varies for random variable with different PDF. In different polynomial chaos methods, the constructed polynomial basis can have a great influence on the accuracy of approximation. For the random variable without

knowing its PDF, MAPC uses the moment of the random variable to construct the polynomial basis, which can avoid the error of approximating the PDF and consequently have a higher accuracy. Note that the moment matrix of statistical data may become indeterminate if very long truncated fat tails are considered [38].

The *n*-degree orthogonal polynomials of MAPC denoted by $\varphi_j(x)$ can be defined by the recurrence relations as follows

$$b_j\varphi_j(x)=(x-a_j)\varphi_{j-1}(x)+b_{j-1}\varphi_{j-2}(x) \tag{20}$$

where, a_j and b_j represents the recurrence coefficient to be estimated. In the framework of MAPC, a_j and b_j can be derived from a Hankel matrix of the random moments. The Hankel matrix of the random moments can be depicted as

$$\mathbf{Q}=\begin{bmatrix} \mu_0 & \mu_1 & \cdots & \mu_p \\ \mu_1 & \mu_2 & & \mu_{p+1} \\ \vdots & & \ddots & \\ \mu_p & \mu_{p+1} & & \mu_{2p} \end{bmatrix} \tag{21}$$

where, μ_k (k = 0 1… 2p) is the statistical moment. μ_k is kth raw moment of the raw data. For a continuous random variable $\gamma^R \in \Omega$ with PDF $\rho(\gamma^R)$, μ_k can be determined by integrating

$$\mu_k = \int_{\gamma^R \in \Omega} (\gamma^R)^k \rho(\gamma^R) d\gamma^R \tag{22}$$

For the set of N samples (random draws or random measurement data) ζ_1, ..., ζ_N, the kth raw moment μ_k can be calculated with

$$\mu_k = \frac{1}{N}\sum_{i=1}^{N} \zeta_i^k \tag{23}$$

Due to the positive definiteness of Hankel matrix, the Cholesky decomposition of **Q** can be computed and depicted as

$$\mathbf{Q} = \mathbf{R}^T \mathbf{R} \tag{24}$$

Explicit analytic formulas have been derived by Rutishauser to obtain the recurrence coefficient from the Cholesky matrix entries **R** [38]. The recurrence coefficients can be expressed as

$$a_j = \frac{r_{j,j+1}}{r_{j,j}} - \frac{r_{j-1,j}}{r_{j-1,j-1}}, \quad b_j = \frac{r_{j+1,j+1}}{r_{j,j}} \tag{25}$$

where, $r_{i,j}$ denotes the elements in **R** with $r_{0,0}$=1 and $r_{0,1}$=0. A more detailed derivation can be found in Ref.[38].

On $\xi \in [-1, 1]$, the polynomial basis obtained through Eq. (20) are orthogonal in regard to the weight function $\varphi_i(\xi)$, and the relations are as follows

$$\left\langle \varphi_i(\xi), \varphi_j(\xi) \right\rangle = h_i \delta_{ij} \tag{26}$$

where $h_i = \left\langle \varphi_i^2(\xi) \right\rangle$, δ_{ij} represents the Kronecker delta and $\langle \cdot, \cdot \rangle$ represents the inner product in regard to the PDF of random variable.

Owing to the orthogonality of the polynomial basis, the expansion coefficient y_i in Eq. (19) can be obtained through the following equation [43].

$$y_i = \frac{\left\langle Y(\xi), \varphi_i(\xi) \right\rangle}{\left\langle \varphi_i(\xi), \varphi_i(\xi) \right\rangle} = \frac{1}{h_i} \int_R Y(\xi) \varphi_i(\xi) w(\xi) d\xi \tag{27}$$

The integral above can be estimated by using the Gauss integration formula and depicted as

$$y_i = \frac{1}{h_i} \int_R Y(\xi) \varphi_i(\xi) w(\xi) d\xi = \frac{1}{h_i} \sum_{i=1}^{m} Y\left(\hat{\xi}_i\right) \varphi_i\left(\hat{\xi}_i\right) w_i \tag{28}$$

Where, $\hat{\xi}_i$ and w_i are the nodes and weights of the Gauss integration rule, respectively; *m* is the total number of Gauss nodes; $\hat{\xi}_i$ and w_i can be obtained from the eigenvalue decomposition of the Jacobi matrix assembled with the recurrence

coefficients of monic orthogonal polynomials. The Jacobi matrix $\mathbf{J}_n$ assembled with the recurrence coefficients a_i and b_i can be expressed as

$$\mathbf{J}_n = \begin{bmatrix} a_0 & b_1 & & & \\ b_1 & a_1 & b_2 & \ddots & \\ & b_2 & \ddots & & \\ & & \ddots & a_{n-2} & b_{n-1} \\ & & & b_{n-1} & a_{n-1} \end{bmatrix} \tag{29}$$

The eigenvalue decomposition of the real symmetric matrix $\mathbf{J}_n$ can be expressed as

$$\begin{aligned} &\mathbf{V}^{\mathrm{T}}\mathbf{J}_n\mathbf{V} = diag\left(\lambda_1, \lambda_2, \ldots, \lambda_n\right) \\ &\mathbf{V}^{\mathrm{T}}\mathbf{V} = \mathbf{I} \end{aligned} \tag{30}$$

Where $\mathbf{I}$ is the $n \times n$ dimension identity matrix. Then, the nodes and weights can be determined by

$$x_i = \lambda_i, \quad w_i = b_0 v_{i,1}^2, \quad i = 1, 2, \ldots \tag{31}$$

in which $v_{i,1}$ is the first element of the *i*th column vector of $\mathbf{V}$.

The expansion coefficient and polynomial basis for fuzzy variable can be calculated refer to Eq. (19-31). The difference is the calculation of μ_k. The polynomial chaos expansion can achieve an excellent accuracy for the fuzzy analysis when the polynomial basis is orthogonal to the weight function of Chebyshev polynomial [44]. Thus, for the fuzzy variable $\gamma^F \in \Omega$, the weight function of Chebyshev polynomial is used to calculated μ_k

$$\mu_k = \int_{\gamma^R \in \Omega} (\gamma^F)^k w_C(\gamma^F) d\gamma^F = \int_{\gamma^R \in \Omega} (\gamma^F)^k \frac{1}{\pi\sqrt{1-\gamma^2}} d\gamma^F \tag{32}$$

The calculated polynomial basis will be orthogonal to the weight function of Chebyshev polynomial.

4.2. Fuzzy and random moment-based arbitrary polynomial chaos method

In the composite structural-acoustic system with fuzzy and bounded random variables, the equivalent macro material properties of the microstructure could express uncertainty because its constituent material properties are uncertain. Namely, the uncertainty at micro-scale propagates to macro-scale through the homogenization process, which result in uncertain equivalent macro material properties. On the other hand, the uncertainties at macro-scale which come from the macro dimension of the structural domain, the physical parameters of the acoustic medium and the external load should also be considered. During the analysis process, the structural-acoustic dynamic stiffness matrix and the load vector are associated with all of these uncertainties at the macro scale. Traditional hybrid uncertain polynomial chao analysis methods are generally based on the gPC or the original APC. These hybrid uncertain polynomial chao analysis methods need to obtain the PDF to yield the fuzzy expectation and variance of the response. In this paper, a new hybrid uncertain analysis method named *fuzzy and random moment-based arbitrary polynomial chaos method* (FRMAPCM) is proposed based on the MAPC. The main advantage of FRMAPCM is that only the moment of random variable is needed. This indicates that the polynomial basis of polynomial can be directly obtained based on the raw data, which can avoid the errors generated by the construction of the PDF of random variable.

In the FRMAPCM, the response of the composite structural-acoustic system with fuzzy and bounded random variables can be approximated as

$$U_k = U_k(\mathbf{x}^F, \mathbf{x}^R) = \sum_{i_1=0}^{N_1} \cdots \sum_{i_L=0}^{N_L} f^k_{i_1,\ldots,i_L} \varphi_{i_1,\ldots,i_{L_1}}(\mathbf{x}^F) \varphi_{i_{L_1+1},\ldots,i_L}(\mathbf{x}^R) \qquad k = 1,2,..,N_{tot} \tag{33}$$

Where

$$f^k_{i_1,\ldots,i_L} \approx \frac{1}{h_1 \times \cdots \times h_L} \sum_{j_1=1}^{M_1} \cdots \sum_{j_L=1}^{M_L} U_k(\hat{\mathbf{x}}^F, \hat{\mathbf{x}}^R) \varphi_{i_1,\ldots,i_{L_1}}(\hat{\mathbf{x}}^F) \varphi_{i_{L_1+1},\ldots,i_L}(\hat{\mathbf{x}}^R) w_{i_1,\ldots,i_L} \tag{34}$$

In the above equation, $\hat{\mathbf{x}}^F$ and $\hat{\mathbf{x}}^R$ denote the integration nodes related to the fuzzy variables and bounded random variables, respectively.

The response analysis of the hybrid uncertain structure-acoustic system includes two main steps. In the first step, the fuzzy variables are regarded as constant parameters, and the response of hybrid uncertain structure-acoustic system can be rewritten as the following form

$$\begin{aligned} U_k &= \sum_{i_{L_1+1}=0}^{N_{L_1+1}} \cdots \sum_{i_L=0}^{N_L} \left(\sum_{i_1=0}^{N_1} \cdots \sum_{i_{L_1}=0}^{N_{L_1}} f^k_{i_1,\ldots,i_L} \varphi_{i_1,\ldots,i_{L_1}}(\mathbf{x}^F) \right) \varphi_{i_{L_1+1},\ldots,i_L}\left(x^R\right) \\ &= \sum_{i_{L_1+1}=0}^{N_{L_1+1}} \cdots \sum_{i_L=0}^{N_L} z^k_{i_{L_1+1},\ldots,i_L} \varphi_{i_{L_1+1},\ldots,i_L}(\mathbf{x}^R) \end{aligned} \tag{35}$$

Where

$$z^k_{i_{L_1+1},\ldots,i_L} = \sum_{i_1=0}^{N_1} \cdots \sum_{i_{L_1}=0}^{N_{L_1}} f^k_{i_1,\ldots,i_L} \varphi_{i_1,\ldots,i_{L_1}}(\mathbf{x}^F) \tag{36}$$

Owing to the orthogonal relationship of the polynomial basis [31], the fuzzy expectation and the variance of the response can be finally obtained as follows

$$\mu_{U_k} = E\left[\sum_{i_{L_1+1}=0}^{N_{L_1+1}} \cdots \sum_{i_L=0}^{N_{L_1}} z^k_{i_{L_1+1},\ldots,i_L} \varphi_{i_{L_1+1},\ldots,i_L}(\mathbf{x}^R) \right] = z^k_{0,\ldots,0} \tag{37}$$

$$\begin{aligned} \sigma^2_{U_k} &= E\left[\left(\sum_{i_{L_1+1}=0}^{N_{L_1+1}} \cdots \sum_{i_L=0}^{N_{L_1}} z^k_{i_{L_1+1},\ldots,i_L} \varphi_{i_{L_1+1},\ldots,i_L}(\mathbf{x}^R) \right)^2 \right] - \left(\mu_{U_k}\right)^2 \\ &= \sum_{i_{L_1+1}=0}^{N_{L_1+1}} \cdots \sum_{i_L=0}^{N_{L_1}} \left(z^k_{i_{L_1+1},\ldots,i_L} \right)^2 h_{i_{L_1+1}} \cdots h_{i_L} - \left(z^k_{0,\ldots,0} \right)^2 \end{aligned} \tag{38}$$

By substituting Eq. (36) into Eq. (37) and Eq. (38), the fuzzy expectation and variance of the response can be rewritten as

$$\mu_{U_k} = \mu_{U_k}(\mathbf{x}^F) = \sum_{i_1=0}^{N_1} \cdots \sum_{i_{L_1}=0}^{N_{L1}} f^k_{i_1,\ldots,i_{L_1},0\ldots,0} \varphi_{i_1,\ldots,i_{L_1}}(\mathbf{x}^F) \tag{39}$$

$$\begin{aligned} \sigma^2_{U_k} = \sigma^2_{U_k}(\mathbf{x}^F) = & \sum_{i_{L_1+1}=0}^{N_{L_1+1}} \cdots \sum_{i_L=0}^{N_L} \left(\sum_{i_1=0}^{N_1} \cdots \sum_{i_{L_1}=0}^{N_{L_1}} f^k_{i_1,\ldots,i_L} \varphi_{i_1,\ldots,i_L}(\mathbf{x}^F) \right)^2 h_{i_{L_1+1}} \cdots h_{i_L} \\ & - \left(\sum_{i_1=0}^{N_1} \cdots \sum_{i_{L_1}=0}^{N_{L_1}} f^k_{i_1,\ldots,i_{L_1},0\ldots,0} \varphi_{i_1,\ldots,i_L}(\mathbf{x}^F) \right)^2 \end{aligned} \tag{40}$$

It is noted here that the fuzzy expectation and variance of the response are approximated by simple functions in terms of the fuzzy parameters. In this paper, the fuzzy variables are defined as *L-R* form. Each λ-cut of μ_{U_k} or $\sigma^2_{U_k}$ can be considered as an interval variable. Therefore, for a given λ-cut, $(\mu_{U_k})^{(\lambda)}$ and $(\sigma^2_{U_k})^{(\lambda)}$ can be regarded as simple functions in terms of the interval variables, and the additional computational cost of the Monte Carlo simulation is acceptable.

Thus, the lower and upper bounds of the fuzzy expectation and variance at each λ-cut can be calculated by the Monte Carlo simulation and expressed as

$$\begin{aligned} \left[\underline{(\mu_{U_k})^{(\lambda)}}, \overline{(\mu_{U_k})^{(\lambda)}} \right] &= \left[\min_{(\mathbf{x}^F)^{(\lambda)} \in Y} \left\{ \mu_{U_k}((\mathbf{x}^F)^{(\lambda)}) \right\}, \max_{(\mathbf{x}^F)^{(\lambda)} \in Y} \left\{ \mu_{U_k}((\mathbf{x}^F)^{(\lambda)}) \right\} \right], \\ \left[\underline{(\sigma^2_{U_k})^{(\lambda)}}, \overline{(\sigma^2_{U_k})^{(\lambda)}} \right] &= \left[\min_{(\mathbf{x}^F)^{(\lambda)} \in Y} \left\{ \sigma^2_{U_k}((\mathbf{x}^F)^{(\lambda)}) \right\}, \max_{(\mathbf{x}^F)^{(\lambda)} \in Y} \left\{ \sigma^2_{U_k}((\mathbf{x}^F)^{(\lambda)}) \right\} \right] \end{aligned} \tag{41}$$

where $Y = \left[\underline{(\mathbf{x}^F)^{(\lambda)}}, \overline{(\mathbf{x}^F)^{(\lambda)}} \right]$, and $(\mathbf{x}^F)^{(\lambda)}$ indicates the λ-cut of $\mathbf{x}^F$.

5. Numerical examples

In this section, a numerical example and two engineering examples are presented to verify the effectiveness of the proposed method for dealing with uncertainty propagation of hybrid fuzzy and bounded random uncertainties. In these numerical

examples, only the statistical data of the random variable is available.

5.1. A simple function

In this case, a simple function is defined to examine the accuracy of the proposed method. For brevity but without loss of generality, the function is defined as

$$y=\exp(x_1^2+x_2^2+x_3^2) \tag{42}$$

where, x_i (i = 1, 2, 3) are dimensionless uncertain variables. x_1 is a fuzzy variable and it's assumed as a linear function of the unitary fuzzy variable ξ_1. x_2 and x_3 are bounded random variables. They are assumed as linear functions of unitary bounded random variables ξ_2 and ξ_3, respectively. These three unitary variables are defined on [−1, 1].

$$\begin{aligned} x_1 &= 1+0.2\xi_1 \\ x_2 &= 1+0.2\xi_2 \\ x_3 &= 1+0.2\xi_3 \end{aligned} \tag{43}$$

It is assumed that ξ_1 is an *L*-*R* fuzzy variable while ξ_2 and ξ_3 are bounded random variable. The reference function of the *L*-*R* fuzzy number $\tilde{I}=(m,\alpha,\beta)_{LR}$ is set as

$$\begin{cases} L(x)=\begin{cases} \dfrac{x-m}{\alpha}+1, & m-\alpha<x\le m \\ 0, & x\le m-\alpha \end{cases} \\ R(x)=\begin{cases} \dfrac{m-x}{\beta}+1, & m\le x<m+\beta \\ 0, & x\le m+\beta \end{cases} \end{cases} \tag{44}$$

When $\lambda\in[0,1]$, the interval of the λ-cut can be depicted as

$$\tilde{I}_\lambda=[m+\alpha(\lambda-1),m-\beta(\lambda-1)] \tag{45}$$

Where, *m* is the main value of $\tilde{I}$. According to the variation range of ξ_1, these parameters can be calculated as follows

$$m=0,\alpha=1,\beta=1 \tag{46}$$

Then, the λ-cut of *L*-*R* fuzzy number ξ_1 can be expressed as

$$\xi_\lambda=[\lambda-1,1-\lambda] \tag{47}$$

The statistical data of ξ_2 and ξ_3 is shown in Fig.1.

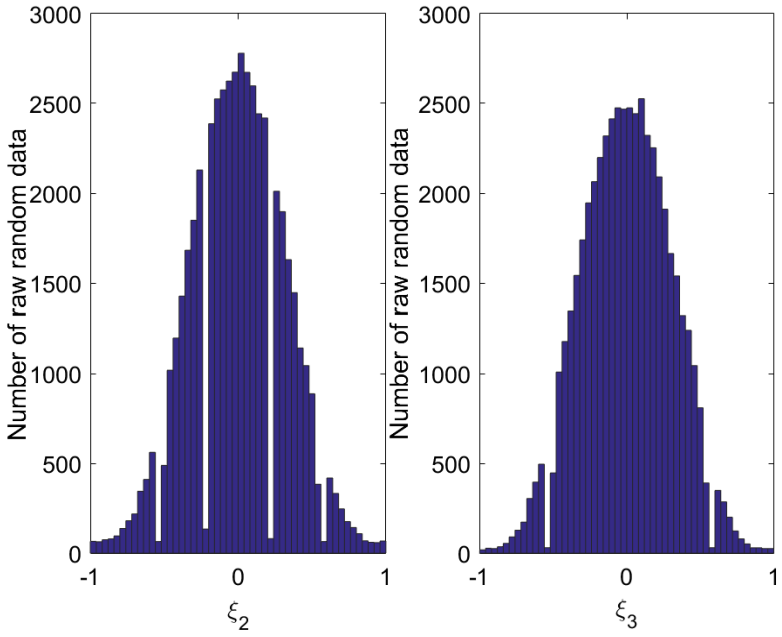

Fig.1 The statistical data of ξ_2 and ξ_3.

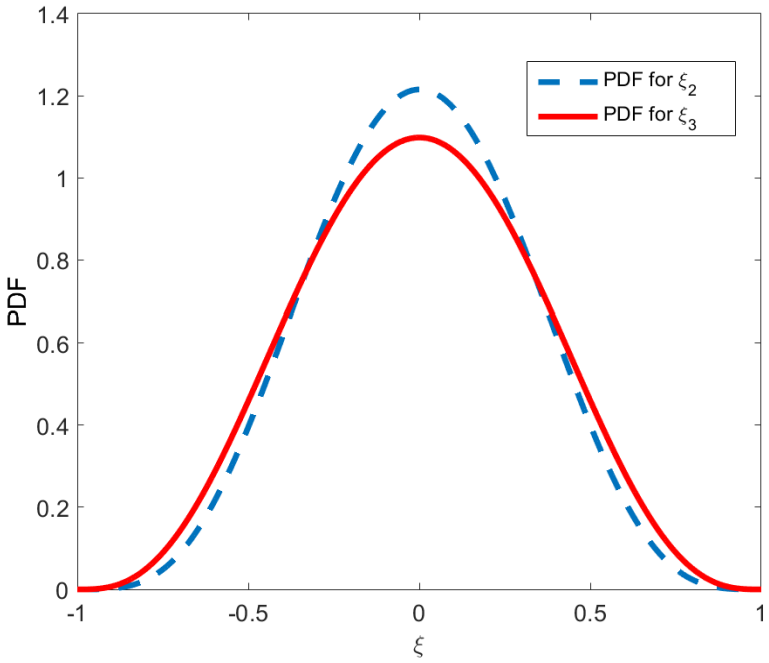

Fig.2 The estimated PDFs for ξ_2 and ξ_3.

The proposed *fuzzy and random moment-based arbitrary polynomial chaos method* (FRMAPCM) method is employed to calculate the response of the simple function defined above. The retained order of FRMAPCM for each random parameter is 4. For comparison, the *fuzzy and random generalized polynomial chaos method* (FRgPCM) [30] and the *Gegenbauer series expansion method* (GSEM) are also introduced to calculate the response of this simple function. Without losing the fairness, the retained order of both FRgPCM and GSEM are chosen to be 4. In FRgPCM, the polynomial basis is constructed according to the PDF of random variable. Therefore, it is necessary to estimate the PDF of the bounded random variables as mentioned above. The PDFs of the bounded random variables of this numerical example are determined by the maximum likelihood estimate method, which are plotted in Fig.2. The reference results are obtained by using the *scanning method and the Monte Carlo method* (SM-MCM). In SM-MCM, 10 uniformly distributed sampling points are used for each λ-cut of fuzzy variable, while 50000 random sampling points are used for the random variable. In this case, simulations of this example are carried out by MATLAB R2015b on a 2.5GHz Core (TM) 4 CPU i5-7300HQ.

The fuzzy expectation and variance of response computed by the proposed FRMAPCM is depicted in Fig.3. The results calculated by FRgPCM and GSEM are also given. From Fig.3, it can be seen apparently that the bounds of the fuzzy variances calculated using the FRgPCM and the GSEM deviate significantly from the

reference results obtained via the SM-MCM, although the bounds of the fuzzy expectations calculated by the FRgPCM and GSEM have a good agreement with the reference results. Whereas, both the bounds of the fuzzy expectation and the bounds of the fuzzy variance calculated by the FRMAPCM match the reference results perfectly. It can also be seen from the results that the accuracy of GSEM is worse than FRgPCM. Therefore, the GSEM is not used as a comparison method in the following numerical examples. The relative error of the fuzzy expectation and variance of response is used to further evaluate the accuracy of the proposed method. The relative error of the fuzzy expectation and variance of response yielded by FRMAPCM and FRgPCM with the same retained order are listed in Table 1-2. It can be observed from Table 1-2 that the FRMAPCM can achieve a better accuracy than the FRgPCM. For FRMAPCM, the relative errors of the obtained bounds of fuzzy variance can maintain at a very small value when λ varies from 0 to 1. However, the relative errors of the bounds of fuzzy variance yielded by FRgPCM are tremendously large, which means that the results obtained by the FRgPCM are unreliable. That is to say, the accuracy of the proposed FRMAPCM is much higher than the FRgPCM when the bounded random variables have only the raw random data.

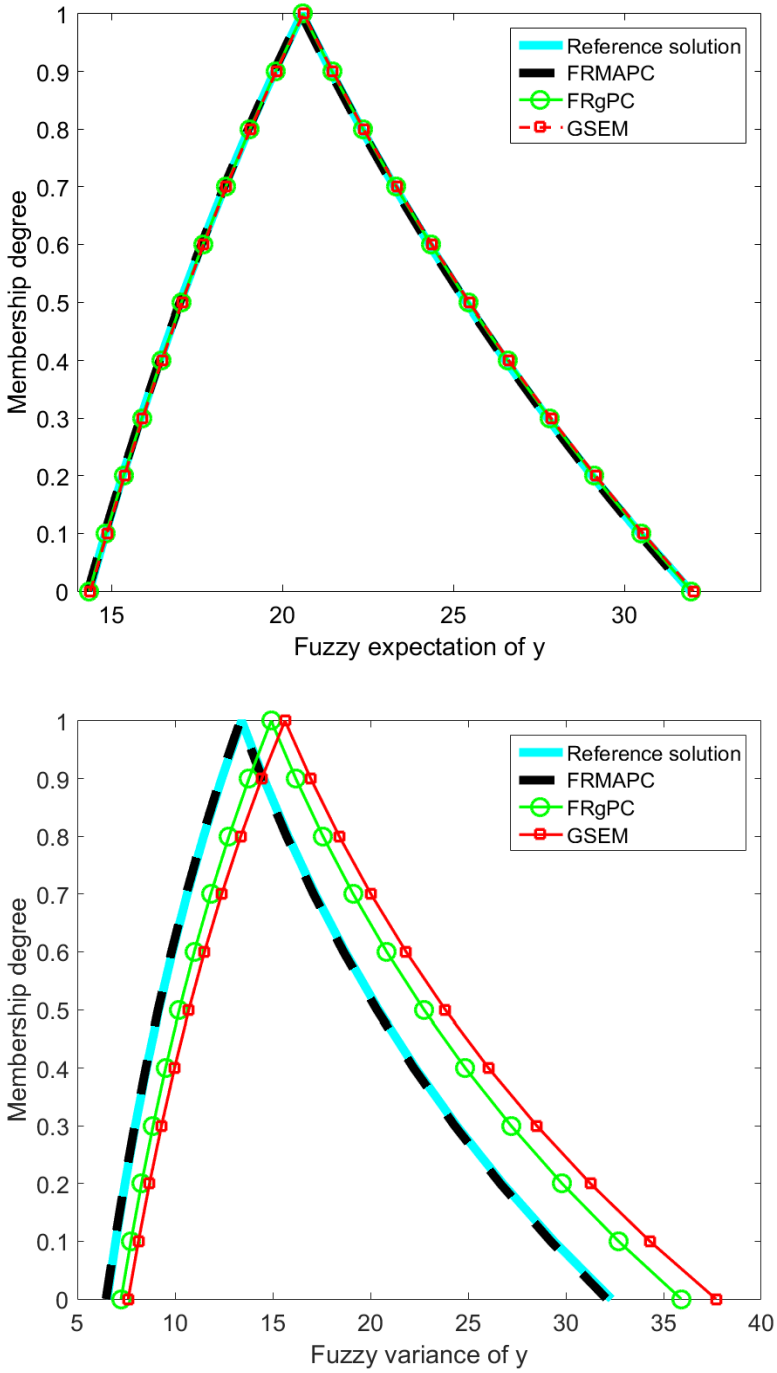

Fig.3 The fuzzy expectation and variance of *y*

Table 1 The relative error of the fuzzy expectation of *y* yielded by FRMAPCM and FRgPCM.

λ	Bound	Reference	FRMAPCM	Error	FRgPCM	Error
0	*Upper*	31.9365	31.9110	0.0799%	31.9970	0.1893%
	Lower	14.3500	14.3386	0.0797%	14.3771	0.1886%

0.2	*Upper*	29.0597	29.0365	0.0798%	29.1151	0.1906%
	Lower	15.3229	15.3107	0.0798%	15.3522	0.1907%
0.4	*Upper*	26.5267	26.5055	0.0798%	26.5772	0.1903%
	Lower	16.4143	16.4012	0.0798%	16.4455	0.1903%
0.6	*Upper*	24.2921	24.2727	0.0798%	24.3383	0.1902%
	Lower	17.6397	17.6256	0.0798%	17.6732	0.1901%
0.8	*Upper*	22.3171	22.2992	0.0798%	22.3595	0.1904%
	Lower	19.0173	19.0022	0.0798%	19.0535	0.1904%
1	*Upper*	20.5683	20.5519	0.0798%	20.6075	0.1906%

Table 2 The relative error of the fuzzy variance of *y* yielded by FRMAPCM and FRgPCM.

λ	Bound	Reference	FRMAPCM	Error	FRgPCM	Error
0	*Upper*	32.3350	32.1768	0.4892%	35.9998	11.3341%
	Lower	6.5283	6.4964	0.4888%	7.2681	11.3325%
0.2	*Upper*	26.7718	26.6409	0.4891%	29.8069	11.3369%
	Lower	7.4436	7.4071	0.4891%	8.2874	11.3372%
0.4	*Upper*	22.3081	22.1990	0.4891%	24.8370	11.3362%
	Lower	8.5416	8.4998	0.4891%	9.5099	11.3362%
0.6	*Upper*	18.7080	18.6165	0.4891%	20.8287	11.3359%
	Lower	9.8646	9.8163	0.4891%	10.9828	11.3358%
0.8	*Upper*	15.7896	15.7123	0.4891%	17.5795	11.3364%
	Lower	11.4656	11.4095	0.4891%	12.7654	11.3364%
1	*Upper*	13.4120	13.3464	0.4891%	14.9325	11.3368%

The *cumulative belief function* (CBF) and the *cumulative plausibility function* (CPF) [28] when the membership degree λ of fuzzy variable is set as 0.5 are also calculated. The results are depicted in Fig.4. It can be seen from Fig.4 that the CBF and CPF calculated by FRMAPC match perfectly with the reference solution. The results calculated by FRgPC obviously deviate from the reference solution.

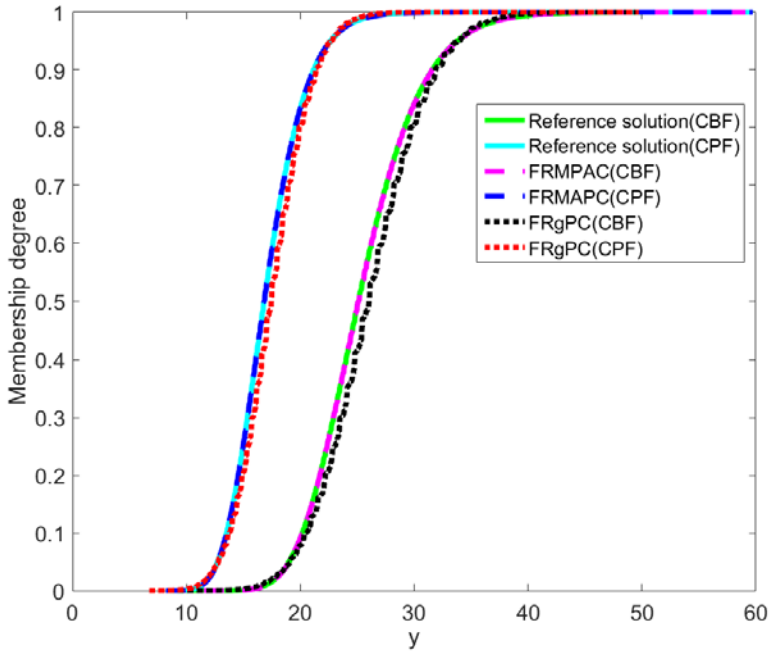

Fig.4 The CBF and CPF of y when $\lambda = 0.5$.

5.2. A hexahedral box

A cavity enclosed by a hexahedral box of dimensions 0.25m × 0.25m ×0.25m is shown in Fig.5. The acoustic field is surrounded by five rigid walls and a clamped plate. The center of the top surface is excited by a concentrated harmonic load F=10 N. The density of the air is 1.21 kg/m^3, and the sound speed of the air 336.9 m/s. The damping coefficients are set as α=0.5 and β=0.1. The clamped plate is discretized by 64 four-node Kirchhoff plate elements and the acoustic domain is discretized by 512 eight-node hexahedral elements. The central line depicted in Fig.5 is used to observe the sound pressure response in the acoustic field. The x-coordinate of the leftmost point at the central line is 0 mm and the x-coordinate of the rightmost point at the central line is 250 mm.

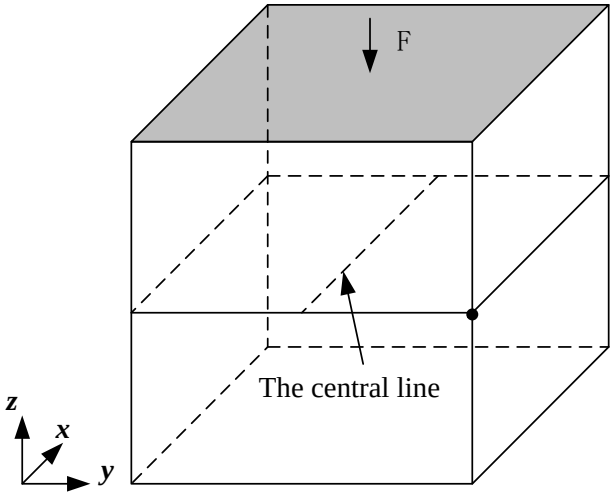

Fig.5 A hexahedral box

The macro clamped plate is composed of a periodic uniform material. The homogenization analysis can be performed to calculate the equivalent macro material properties. A unit *representative volume element* (RVE) of the unidirectional fiber reinforced composite is depicted in Fig.6. For simplicity, it is assumed that the unit cells at the micro scale are square and with a dimensionless length of 1 × 1. The radius of the fiber in the center of the matrix is 0.2. The finite element model of the RVE is composed of 361 nodes and 340 elements. The microstructure unit cell consists of two prescribed materials, namely, the strong material (Red color) and the soft material (Green color). The Young's modulus, mass density and the Poisson's ratio of strong material are E_1 =210 GPa, ρ_1 =7800 kg/m^3 and v_1=0.3, respectively. The soft material in the unit cell has $E_2 = E_1 / 10$, $\rho_2 = \rho_1 / 10$, and $v_2 = 0.3$. The sound speed of the air is assumed as 336.9 m/s.

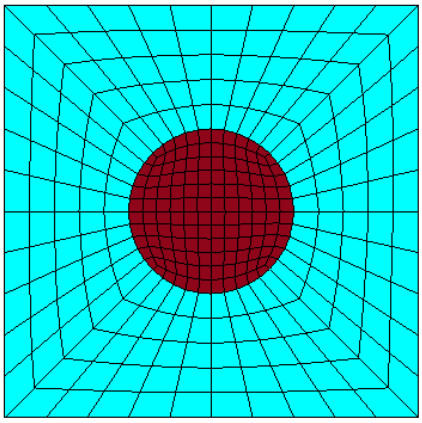

Fig.6 RVE of a unidirectional fiber reinforced composite

At the micro-scale, considering the unpredictability of the material properties, the Young's modulus of the fiber and the matrix are assumed to be bounded random variables, which are $\mathrm{E}_1 = 210 + 42 \times \xi_2 \,\mathrm{GPa}$ and $\mathrm{E}_2 = 21 + 4.2 \times \xi_3 \,\mathrm{GPa}$, respectively. At the macro-scale, the thickness of the plate is assumed to be a fuzzy variable, which is depicted as $\mathrm{t}_1 = 1 + 0.2 \times \xi_1$ mm. The ξ_1, ξ_2 and ξ_3 are defined in Section 5.1. The retained orders for these three variables are set $n_{\mathrm{E}_1} = n_{\mathrm{E}_2} = n_{\mathrm{t}} = 4$. The fuzzy expectation and variance of sound pressure response are calculated by the proposed FRMAPCM. Due to the excessive computation burden of the SM-MCM, the reference results are calculated by Legendre expansion method [**Fehler! Textmarke nicht definiert.**] with high retained order, which is set as 6. Simulations of this hexahedral box are carried out by MATLAB R2015b on a 2.5GHz Core (TM) 4 CPU i5-7300HQ .

In Fig.7 and 8, the fuzzy expectation and variance of sound pressure response computed by the proposed FRMAPCM at the central line when f = 100Hz is depicted. It should be pointed out that the sound pressure in this paper represents the root of the sum of squares of the real and imaginary parts of the sound pressure. The result

calculated by FRgPCM is also given. It can be seen from Fig.7 and 8 that the fuzzy variance of sound pressure obtained by FRMAPCM is very close to the reference results. However, the fuzzy variance of sound pressure obtained through FRgPCM deviates largely from the reference results. Therefore, from these results obtained by the proposed FRMAPCM and FRgPCM for uncertainty analysis of the hexahedral box with bounded random variables and fuzzy variables, it can be concluded that the proposed FRMAPCM can achieve higher accuracy compared with FRgPCM when only the raw random data is available for the random variable.

Additionally, the upper and lower bounds of the sound pressure amplitude at x = 0 mm computed by the FRMAPCM and FRgPCM when $\lambda = 0.5$ are shown in Fig.9 and 10. The considered frequency range is from 50 to 210 Hz. Fig.11 and 12 depicts that the sound pressure calculated by FRMAPCM and FRgPCM at x = 0mm when f = 200Hz and the membership degree λ changes from 0 to 1. The reference solutions are also given in these figures. From these figures, it can be found out that the fuzzy variance of sound pressure obtained by using FRMAPCM is very close to the reference results. As a comparison, the fuzzy variance of sound pressure obtained by FRgPCM deviates largely from the reference results. This further indicates that the proposed FRMAPCM can achieve higher accuracy than the FRgPCM when only raw random data for the random variable is acquired.

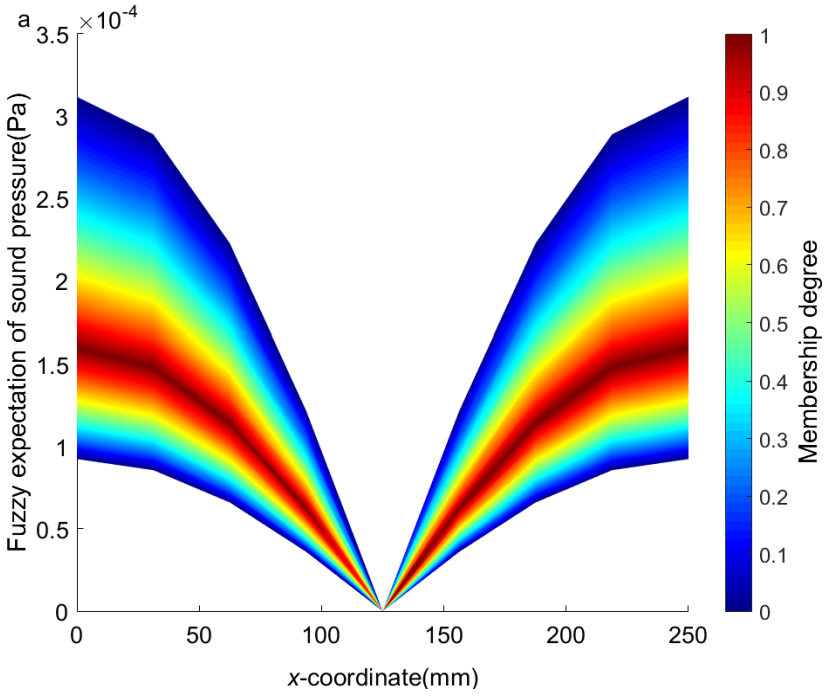
a
×10^-4
3.5
3
2.5
2
1.5
1
0.5
0
Fuzzy expectation of sound pressure(Pa)
0
50
100
150
200
250
x-coordinate(mm)
1
0.9
0.8
0.7
0.6
0.5
0.4
0.3
0.2
0.1
0
Membership degree

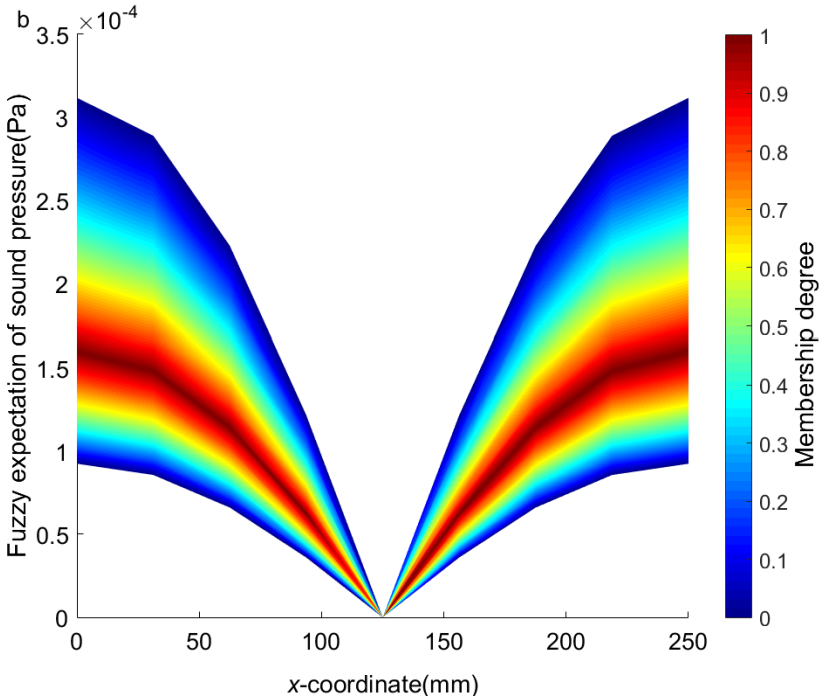
b
×10^-4
3.5
3
2.5
2
1.5
1
0.5
0
Fuzzy expectation of sound pressure(Pa)
0
50
100
150
200
250
x-coordinate(mm)
1
0.9
0.8
0.7
0.6
0.5
0.4
0.3
0.2
0.1
0
Membership degree

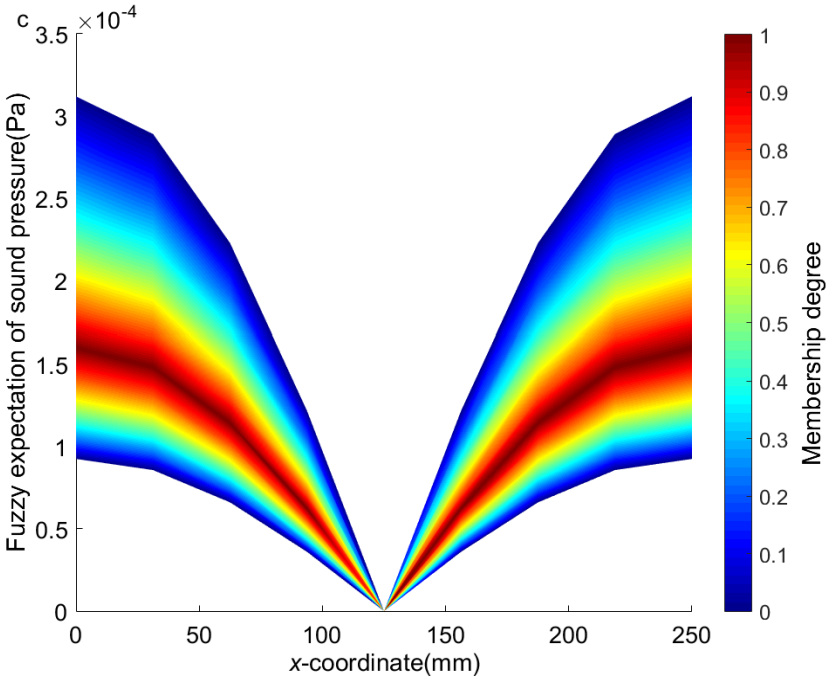

Fig.7 The fuzzy expectation of sound pressure for f = 200Hz at the central line (a. Reference solution; b. FRMAPCM; c. FRgPCM)

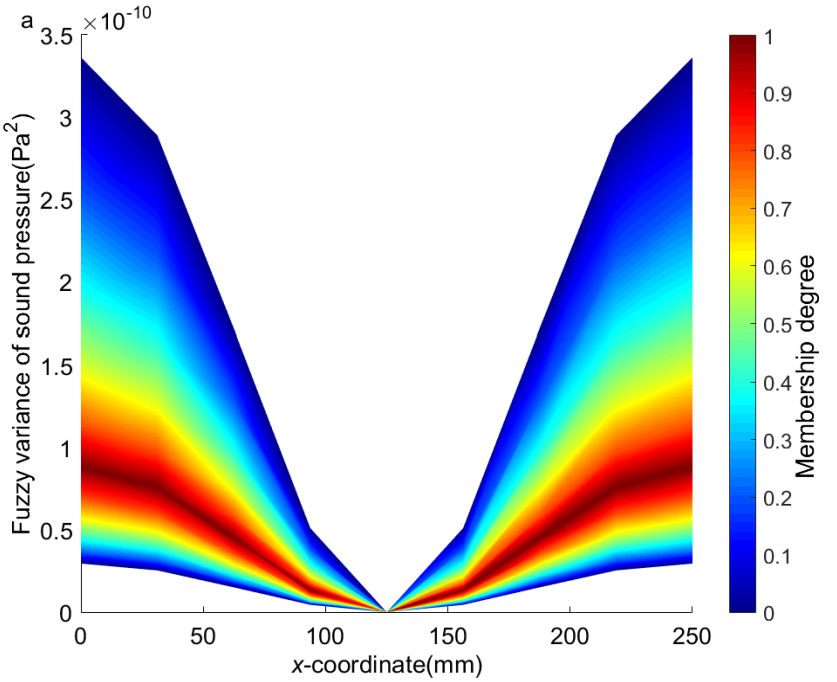

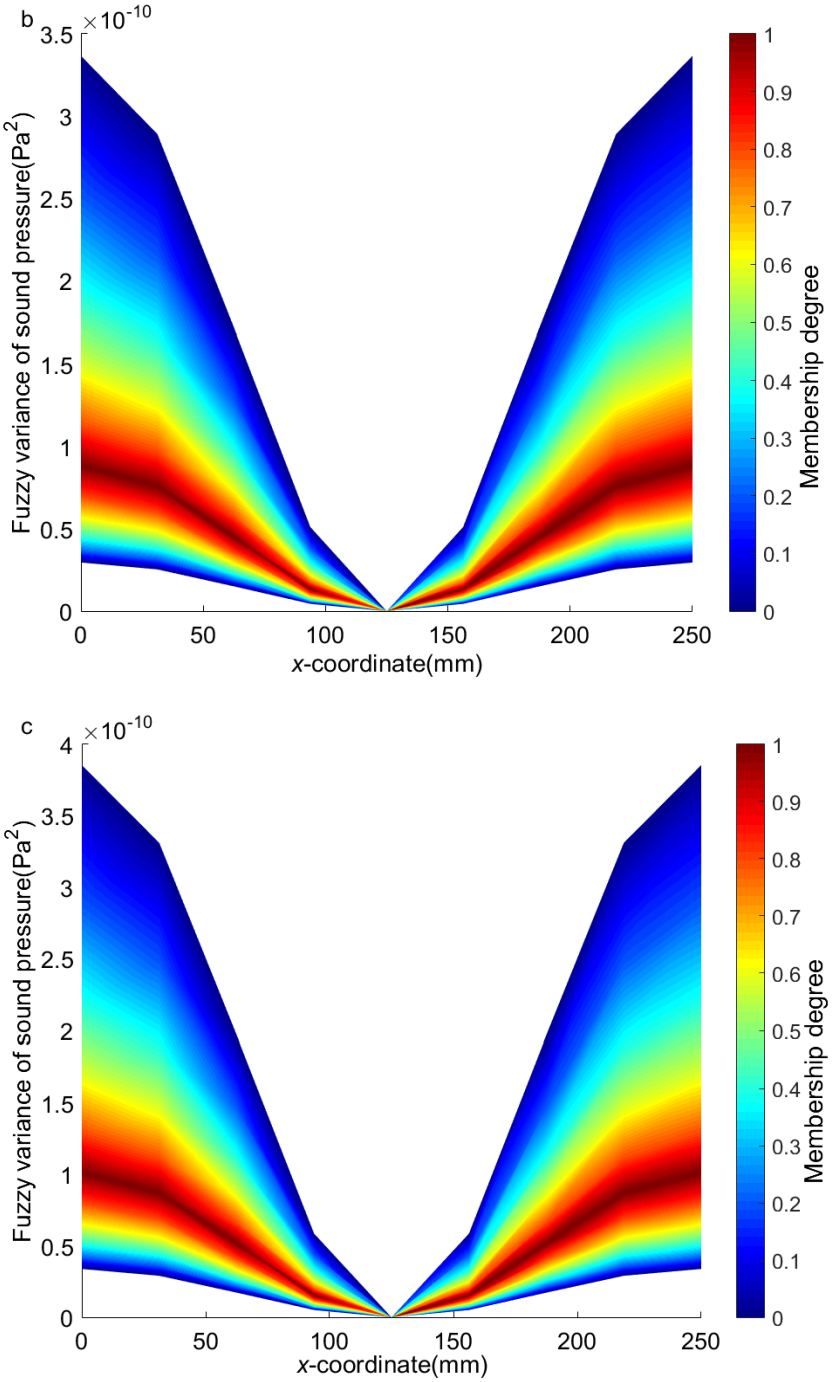

Fig.8 The fuzzy variance of sound pressure for f = 200Hz at the central line (a. Reference solution;

b. FRMAPCM; c. FRgPCM)

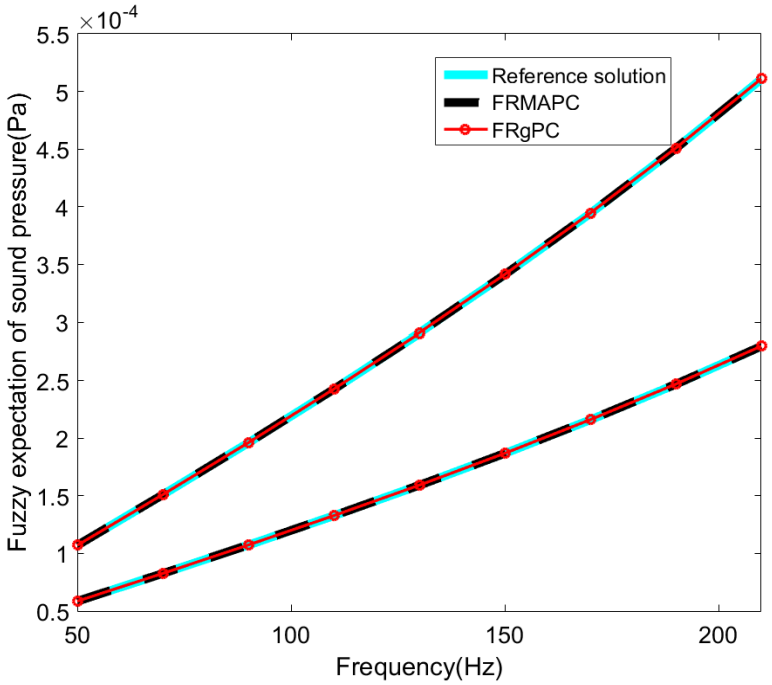

Fig.9 The fuzzy expectation of sound pressure at the x = 0mm (f = 50-200Hz and λ=[0,1])

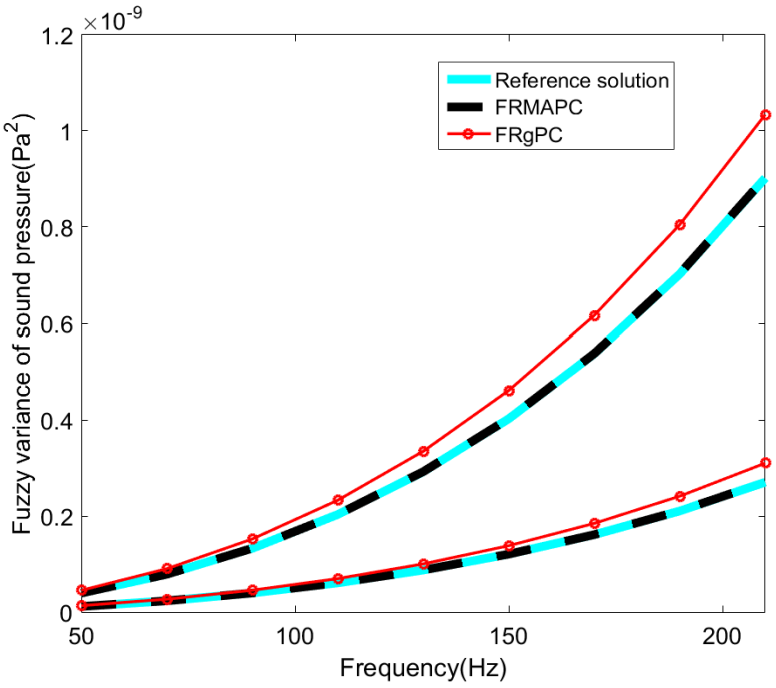

Fig.10 The fuzzy variance of sound pressure at the x = 0mm (f = 50-200Hz and λ=[0,1])

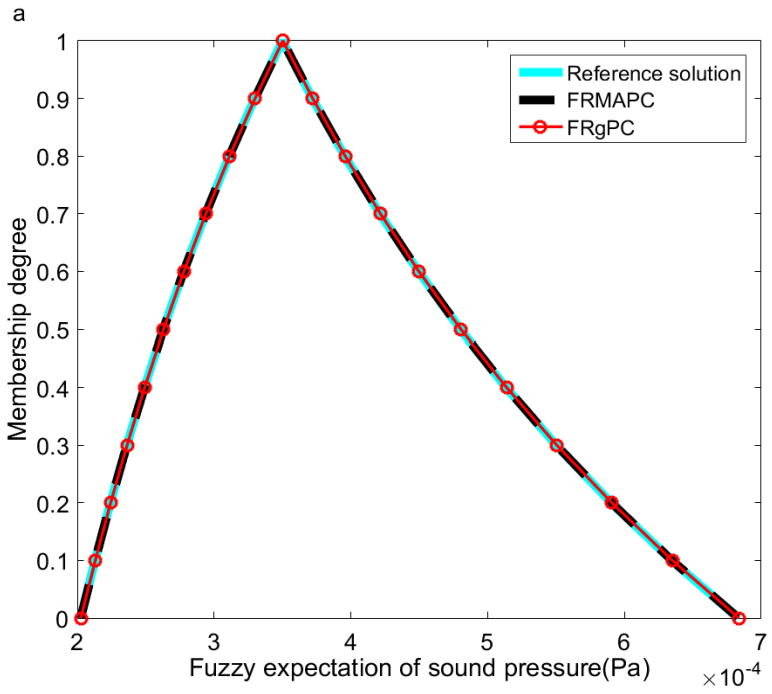

Fig.11 The fuzzy expectation of sound pressure at the x = 0mm (f = 200Hz and λ=[0,1])

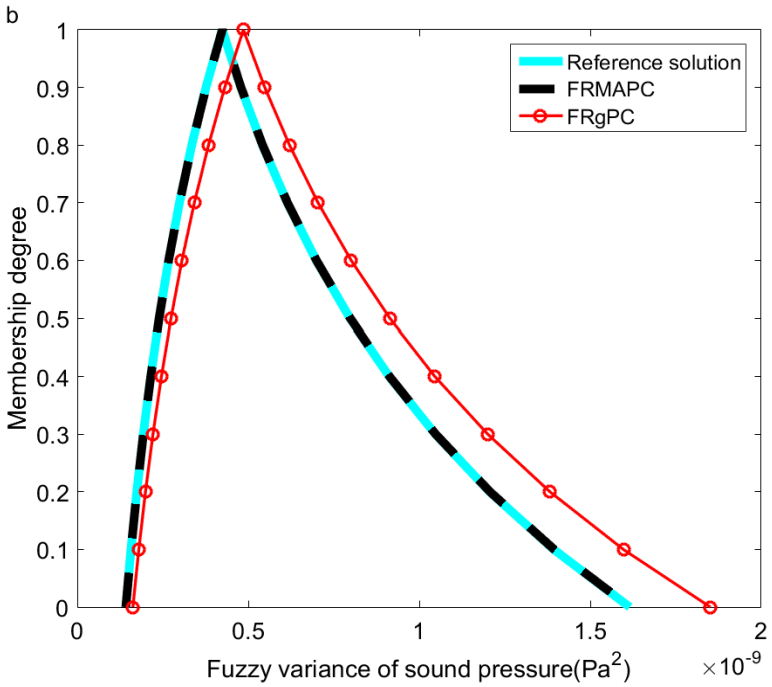

Fig.12 The fuzzy variance of sound pressure at the x = 0mm (f = 200Hz and λ=[0,1])

5.3. An automobile passenger compartment

Fig.13 depicts an automobile passenger compartment with flexible roof panel. The roof is excited by a unit normal harmonic point force at the center. The thickness

of the roof panel is 1 mm. The four sides of the roof panel are set to be fixed. The density and the sound speed of the air are 1.21 kg/m^3 and 336.9 m/s, respectively. The node A is near the driver's left ear. The macro roof panel is assumed to be composed of a periodic uniform material. The microstructure unit cell consists of two prescribed materials. The two materials employed, and the unit RVE of the unidirectional fiber reinforced composite are the same as those in Section 5.2. At the micro-scale, considering the unpredictability of the material properties, the Young's modulus of the fiber and the matrix are assumed to be bounded random variables, which are $\mathrm{E}_1 = 210 + 42 \times \xi_2$ GPa and $\mathrm{E}_2 = 21 + 4.2 \times \xi_3$ GPa, respectively. At the macro-scale, the thickness of the plate is assumed to be a fuzzy variable, which is depicted as $\mathrm{t}_1 = 1 + 0.2 \times \xi_1$ mm. The ξ_1, ξ_2 and ξ_3 are defined in Section 5.1. The retained orders for these three variables are set $n_{\mathrm{E}_1} = n_{\mathrm{E}_2} = n_{\mathrm{t}} = 4$. The fuzzy expectation and variance of sound pressure response are calculated using the proposed method. And the result computed by FRgPCM is used as a comparison. Due to the tremendous computational cost of SM-MCM, the result calculated by Legendre expansion method with a high retained order of 6 is regarded as reference solution. Simulations of this automobile passenger compartment are carried out by MATLAB R2015b on a 2.5GHz Core (TM) 4 CPU i5-7300HQ.

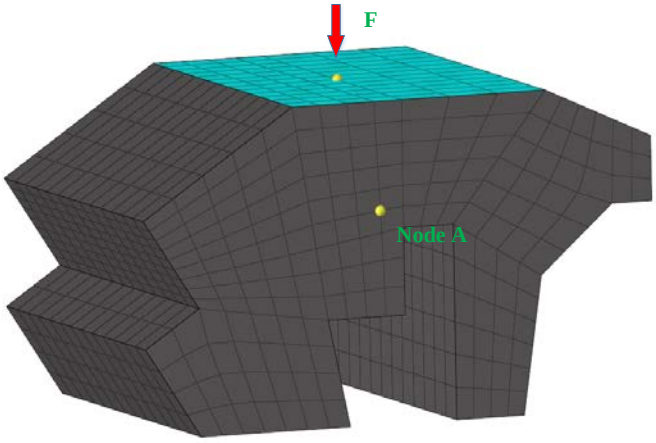

Fig. 13 An automobile passenger compartment

The fuzzy expectation and variance of sound pressure response at node A when f = 50-210Hz computed by the proposed method are depicted in Fig.14 and 15. The result calculated by FRgPCM is also given. It can be seen from Fig.14 and 15 that the fuzzy variance of sound pressure obtained by FRMAPCM have a great agreement with the reference solution. In contrast, there is a large deviation between the fuzzy variance of sound pressure obtained by the FRgPCM and the reference solution. Then, it can be concluded from the application of the proposed FRMAPCM and FRgPCM for uncertainty analysis of the automobile passenger compartment with bounded random variables and fuzzy variables that the proposed FRMAPCM can achieve higher accuracy for the structural-acoustic problem when only the raw random data is available for the random variable.

Fig.16 and 17 depicts that the fuzzy expectation and variance of sound pressure calculated by FRMAPCM and FRgPCM at node B when f = 100Hz and the membership degree λ changes from 0 to 1. The fuzzy variance of sound pressure obtained by FRMAPCM matches the reference solution perfectly well. In contrast,

there is a large deviation between the fuzzy variance of sound pressure obtained by the FRgPCM and the reference solution. It further verifies that the proposed FRMAPCM can achieve higher accuracy than the FRgPCM when only raw random data for the random variable is acquired. In addition, the efficiency of the FRMAPCM and the FRgPCM are investigated here. Table 3 shows that the computational time of the proposed FRMAPCM is close to that of FRgPCM. Meanwhile, it can be found out that the execution time of the proposed FRMAPCM and the FRgPCM are much less than that of reference method. This is mainly because the reference method has higher retained order than the FRMAPCM and FRgPCM. The computational burdens of FRMAPCM and FRgPCM mainly concentrate in the calculation of the expansion coefficients related to the multi-dimension polynomial terms. When the same expansion order is retained, the number of multi-dimension polynomial terms of FRMAPCM is the same as that of FRgPCM. As a result, there is almost no difference between FRMAPCM and FRgPCM on efficiency.

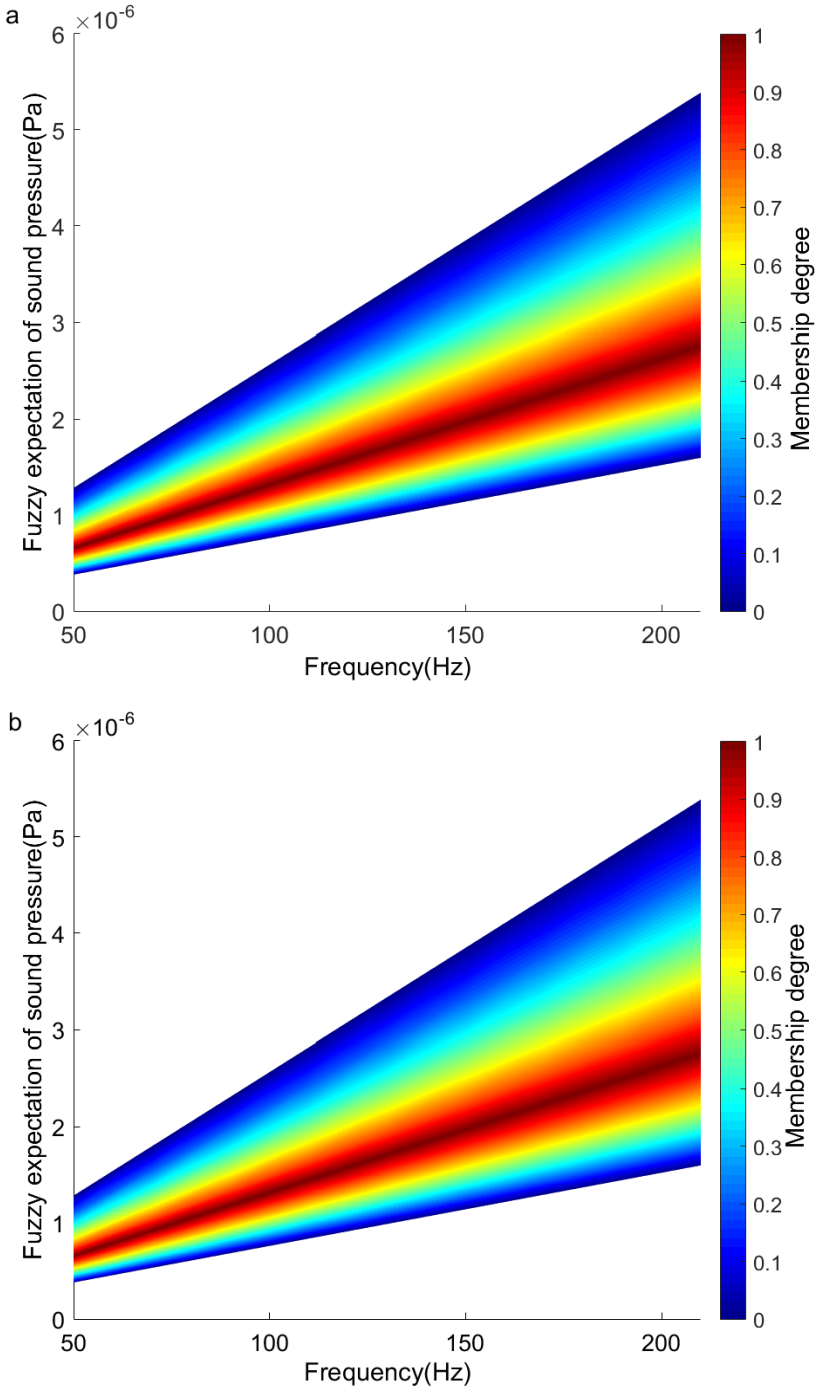
a
×10^-6
Fuzzy expectation of sound pressure(Pa)
Frequency(Hz)
Membership degree
b
×10^-6
Fuzzy expectation of sound pressure(Pa)
Frequency(Hz)
Membership degree

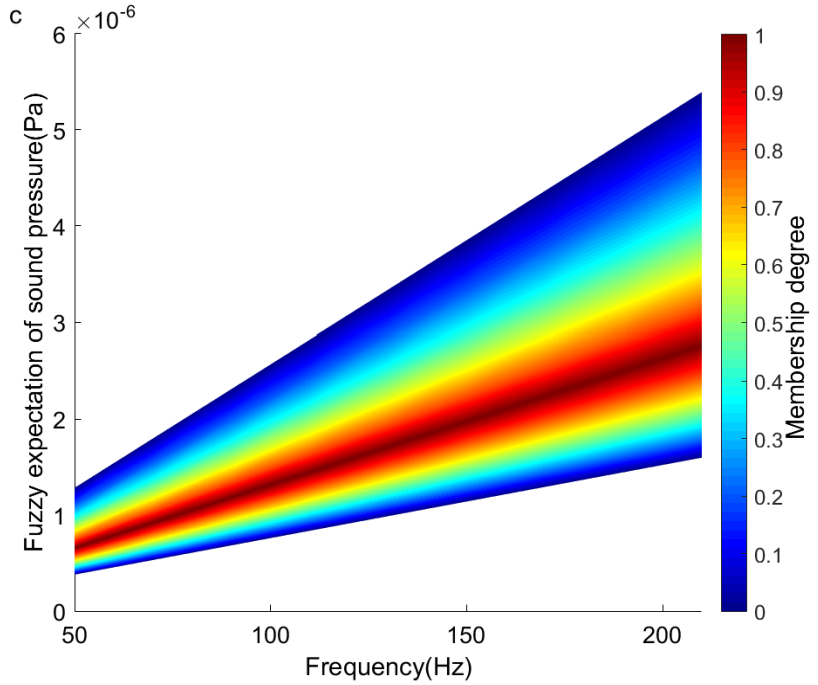

Fig.14 The fuzzy expectation of sound pressure at node A for f = 50-210Hz (a. Reference solution,

b. FRMAPCM, c. FRgPCM)

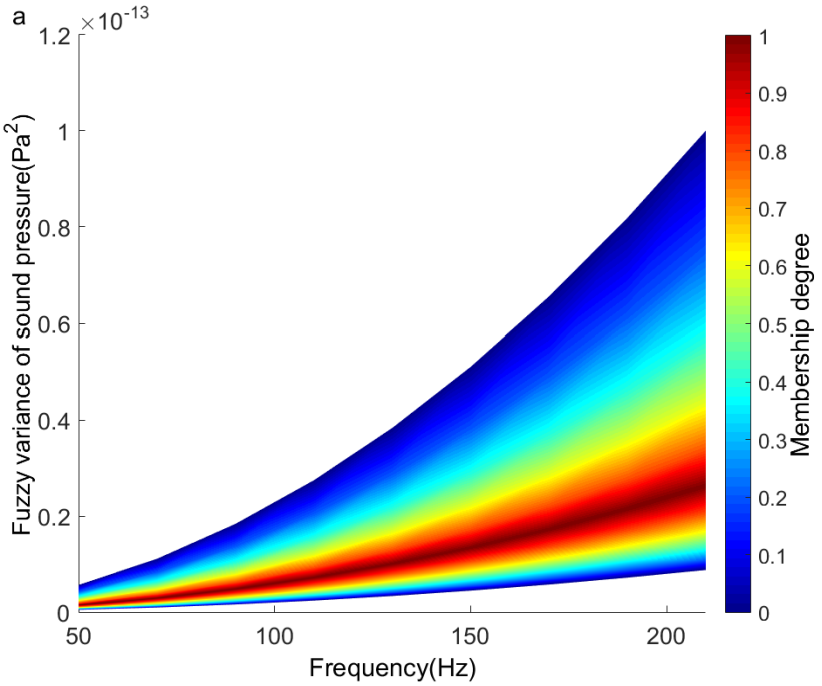

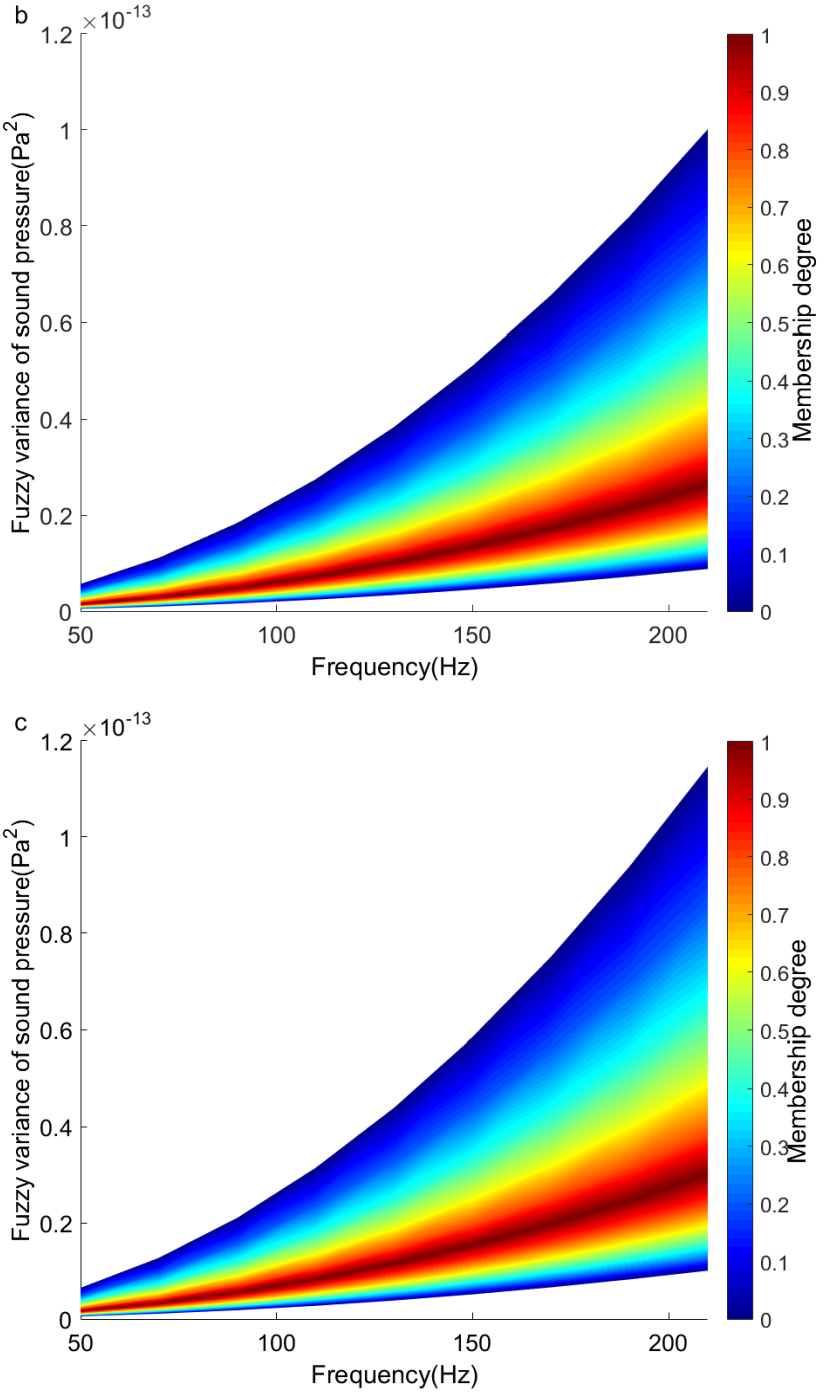

Fig.15 The fuzzy variance of sound pressure at node A for f = 50-210Hz (a. Reference solution, b. FRMAPCM, c. FRgPCM)

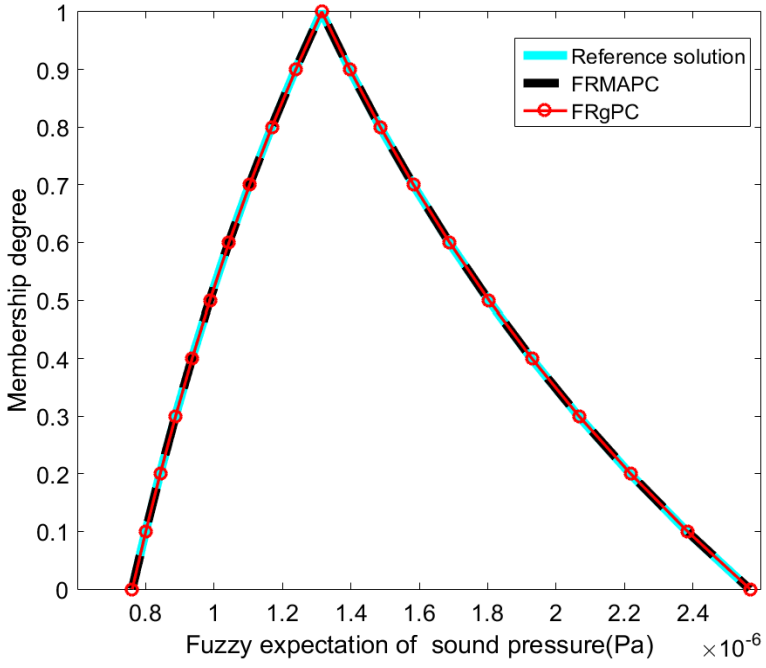

Fig.16 The fuzzy expectation of sound pressure at node A (f = 100Hz and λ=[0,1])

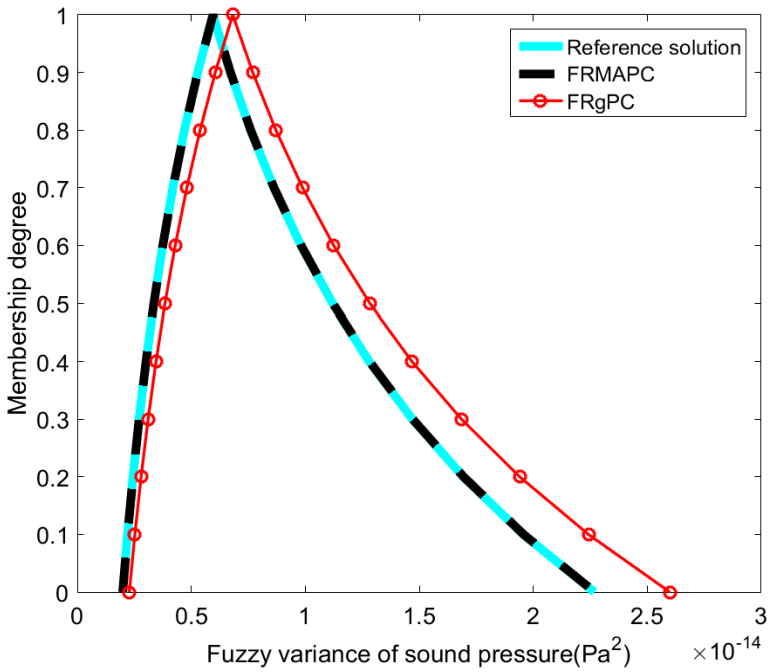

Fig.17 The fuzzy variance of sound pressure at node A (f = 100Hz and λ=[0,1])

Table 3 Execution time of the FRMAPC, FRgPC and the Reference Solution.

Method	FRMAPC	FRgPC	Reference Solution
Execution time	486.4 s	526.5 s	3624.4 s

6. Conclusions

D Due to the inherent variation of the physical system, environment and the incomplete or inaccurate information, the composite structural-acoustic problems are inevitably involved with multi-scale uncertainties in engineering practice. These uncertainties may lead to significant fluctuation of the acoustic behavior of the engineering system. In this paper, the hybrid fuzzy and bounded random model is introduced to describe these uncertainties. The bounded random variables are used to model aleatory uncertainty, whereas the fuzzy variables are used to represent epistemic uncertainty. To efficiently calculate the response of composite structural-acoustic system with multi-scale hybrid fuzzy and bounded random variables, a new method named as *fuzzy and random moment-based arbitrary polynomial chaos method* (FRMAPCM) is presented based on the moment-based arbitrary polynomial chaos. In FRMAPCM, the response of the system with fuzzy and bounded random variables is approximated by the *moment-based arbitrary polynomial chaos* (MAPC) expansion in a unified mathematical framework. The polynomial basis of the MAPC expansion related to the random variable is constructed according to the moment of the random variable rather than the approximate *probability density function* (PDF). The weight function of the Chebyshev polynomial is assumed as the PDF to yield the moment matrix for the fuzzy variable. The proposed FRMAPC has been employed to calculate the fuzzy expectation and variance of the response of a hexahedral box and an automobile passenger compartment with hybrid fuzzy and bounded random variables. The merits

of the proposed method have been demonstrated by comparing it with the *fuzzy and random generalized polynomial chaos method* (FRgPCM) and the *Gegenbauer series expansion method* (GSEM). It can be concluded from these numerical examples that when the exact PDF cannot be obtained based on the raw statistics, the proposed FRMAPCM can achieve better accuracy than FRgPCM and GSEM. Therefore, the FRMAPCM is verified to be a more reliable and promising approach for dealing with uncertainty propagation of hybrid fuzzy and bounded random uncertainties.

Acknowledgments

The paper is supported by the Foundation for Innovative Research Groups of the National Natural Science Foundation of China (Grant No. 51621004), the National Natural Science Foundation of China (Grant No. 51905162), the Natural Science Foundation of Hunan Province (Grant No. 2019JJ50062) and the Fundamental Research Funds for the Central Universities (Grant No. 531107051148). The author would also like to thank reviewers for their valuable suggestions.

References

1. Hoffman, F.O. and J.S. Hammonds, *Propagation of Uncertainty in Risk Assessments: The Need to Distinguish Between Uncertainty Due to Lack of Knowledge and Uncertainty Due to Variability.* Risk Analysis An Official Publication of the Society for Risk Analysis, 1994. **14**(5): p. 707-712.
2. Hurtado, J.E. and A.H. Barbat, *Monte Carlo techniques in computational stochastic mechanics.* Archives of Computational Methods in Engineering, 1998. **5**(1): p. 3-30.
3. Kamiński, M.M., *A generalized stochastic perturbation technique for plasticity problems.* Computational Mechanics, 2010. **45**(4): p. 349.
4. Lazarov, B., M. Schevenels, and O. Sigmund, *Topology optimization with geometric uncertainties by perturbation techniques.* International Journal for Numerical Methods in Engineering, 2012. **90**: p. 1321-1336.
5. Jiang, G.Q., L.Y. Yao, and F. Wu, *A stochastic perturbation finite element-least square point interpolation method for the analysis of uncertain*

structural-acoustics problems with random variables. Applied Acoustics, 2018. **137**: p. 18-26.
6. Xiu, D. and G.E. Karniadakis, *The Wiener--Askey Polynomial Chaos for Stochastic Differential Equations.* Siam Journal on Entific Computing, 2002.
7. Wu, C.L., X.P. Ma, and T. Fang, *A complementary note on Gegenbauer polynomial approximation for random response problem of stochastic structure.* Probabilistic Engineering Mechanics, 2006. **21**(4): p. 410-419.
8. Henneberg, J., et al., *Periodically arranged acoustic metamaterial in industrial applications: The need for uncertainty quantification.* Applied Acoustics, 2020. **157**: p. 107026.
9. Dammak, K., et al., *Numerical modelling of vibro-acoustic problem in presence of uncertainty: Application to a vehicle cabin.* Applied Acoustics, 2019. **144**: p. 113-123.
10. Ben-Haim, Y. and I. Elishakoff, *Convex Models of Uncertainty in Applied Mechanics.* 1990. **25**.
11. Moens, D. and D. Vandepitte, *A survey of non-probabilistic uncertainty treatment in finite element analysis.* Computer Methods in Applied Mechanics & Engineering, 2005. **194**(12/16): p. 1527-1555.
12. Wang, C. and H.G. Matthies, *Hybrid evidence-and-fuzzy uncertainty propagation under a dual-level analysis framework.* Fuzzy Sets & Systems, 2018.
13. Xu, M., et al., *A dual-layer dimension-wise fuzzy finite element method for structural analysis with epistemic uncertainties.* Fuzzy Sets & Systems, 2018. **367**: p. S0165011418305396-.
14. Lü, H., et al., *An improved method for fuzzy–interval uncertainty analysis and its application in brake instability study.* Computer Methods in Applied Mechanics and Engineering, 2018. **342**: p. 142-160.
15. Lü, H., W.-B. Shangguan, and D. Yu, *A unified method and its application to brake instability analysis involving different types of epistemic uncertainties.* Applied Mathematical Modelling, 2018. **56**: p. 158-171.
16. Lü, H., W.-B. Shangguan, and D. Yu, *Uncertainty quantification of squeal instability under two fuzzy-interval cases.* Fuzzy Sets and Systems, 2017. **328**: p. 70-82.
17. Mourelatos, Z.P. and J. Zhou, *Reliability Estimation and Design with Insufficient Data Based on Possibility Theory.* Aiaa Journal, 2005. **43**(8): p. p.1696-1705.
18. McWilliam, S., *Anti-optimisation of uncertain structures using interval analysis.* Computers & Structures, 2001. **79**(4): p. 421-430.
19. Wu, J., et al., *A Chebyshev interval method for nonlinear dynamic systems under uncertainty.* Applied Mathematical Modelling, 2013. **37**(6): p. 4578-4591.
20. Yin, S., et al., *A new evidence-theory-based method for response analysis of acoustic system with epistemic uncertainty by using Jacobi expansion.* Computer Methods in Applied Mechanics & Engineering, 2017. **322**(aug.1): p. 419-440.
21. Qiu, Z. and I. Elishakoff, *Antioptimization of structures with large uncertain-but-non-random parameters via interval analysis.* Computer Methods in Applied Mechanics & Engineering, 1998. **152**(3-4): p. 361-372.

22. Wang, C., Z. Qiu, and Y. Li, *Hybrid uncertainty propagation of coupled structural–acoustic system with large fuzzy and interval parameters.* Applied Acoustics, 2016. **102**: p. 62-70.
23. Long, X.Y., et al., *Unified uncertainty analysis under probabilistic, evidence, fuzzy and interval uncertainties.* Computer Methods in Applied Mechanics & Engineering, 2019. **355**(1): p. 1-26.
24. Lü, H., et al., *An efficient approach for the design optimization of dual uncertain structures involving fuzzy random variables.* Computer Methods in Applied Mechanics and Engineering, 2020. **371**: p. 113331.
25. Lü, H., W.-B. Shangguan, and D. Yu, *A unified approach for squeal instability analysis of disc brakes with two types of random-fuzzy uncertainties.* Mechanical Systems and Signal Processing, 2017. **93**: p. 281-298.
26. Gao, W., C. Song, and F. Tin-Loi, *Probabilistic interval analysis for structures with uncertainty.* Structural Safety, 2010. **32**(3): p. 191-199.
27. Moore, R. and W. Lodwick, *Interval analysis and fuzzy set theory.* Fuzzy Sets & Systems, 2003. **135**(1): p. 5-9.
28. Chen, N., et al., *A polynomial expansion approach for response analysis of periodical composite structural-acoustic problems with multi-scale mixed aleatory and epistemic uncertainties.* Computer Methods in Applied Mechanics & Engineering, 2018. **342**(DEC.1): p. 509-531.
29. Chen, N., et al., *Hybrid interval and random analysis for structural-acoustic systems including periodical composites and multi-scale bounded hybrid uncertain parameters.* Mechanical Systems & Signal Processing, 2019. **115**(JAN.15): p. 524-544.
30. Jacquelin, E., et al., *Polynomial chaos expansion with random and fuzzy variables.* Mechanical Systems & Signal Processing, 2016: p. 41-56.
31. Xiu, D. and G.E. Karniadakis, *Modeling uncertainty in flow simulations via generalized polynomial chaos.* Journal of Computational Physics, 2003. **187**(1): p. 137-167.
32. Gao, R., K. Zhou, and Y. Lin, *A Flexible Polynomial Expansion Method for Response Analysis with Random Parameters.* Complexity, 2018. **2018**: p. 1-14.
33. Qiu, Z. and Z. Zhang, *Fatigue crack propagation analysis in structures with random parameters based on polynomial chaos expansion method.* Theoretical & Applied Fracture Mechanics, 2019. **105**: p. 102404.
34. Xu, M., et al., *A dual-layer dimension-wise fuzzy finite element method (DwFFEM) for the structural-acoustic analysis with epistemic uncertainties.* Mechanical Systems & Signal Processing, 2019. **128**(AUG.1): p. 617-635.
35. Yin, S., et al., *Interval and random analysis for structure–acoustic systems with large uncertain-but-bounded parameters.* Computer Methods in Applied Mechanics & Engineering, 2016. **305**: p. 910-935.
36. Xiu, D. and G.E. Karniadakis, *A new stochastic approach to transient heat conduction modeling with uncertainty.* International Journal of Heat & Mass Transfer, 2003. **46**(24): p. 4681-4693.
37. Yin, S., et al., *Unified polynomial expansion for interval and random response*

analysis of uncertain structure-acoustic system with arbitrary probability distribution. Computer Methods in Applied Mechanics & Engineering, 2018. **336**(jul.1): p. 260-285.
38. Ahlfeld, R., B. Belkouchi, and F. Montomoli, *SAMBA: Sparse Approximation of Moment-Based Arbitrary Polynomial Chaos.* Journal of Computational Physics, 2016. **320**: p. 1-16.
39. Bendsøe, M.P. and N. Kikuchi, *Generating optimal topologies in structural design using a homogenization method.* Computer Methods in Applied Mechanics & Engineering, 1988. **71**(2): p. 197-224.
40. Stefanou, G., *The stochastic finite element method: Past, present and future.* Computer Methods in Applied Mechanics & Engineering, 2009. **198**(9): p. 1031-1051.
41. Hanss, M., *Applied fuzzy arithmetic an introduction with engineering applications.* 2005.
42. Zadeh, L.A., *Fuzzy sets.* Information & Control, 1965. **8**(3): p. 338-353.
43. Gautschi, W. *Orthogonal Polynomials: Computation and Approximation*. in *Numerical Mathematics & Scientific Computation*. 2004.
44. Yin, H., et al., *Possibility-based robust design optimization for the structural-acoustic system with fuzzy parameters.* Mechanical Systems & Signal Processing, 2018. **102**(MAR.1): p. 329-345.